ScienceImmunology

Submitted Manuscript: Confidential template updated: July 5 2016

Title: IL-6 effector function of group-2 innate lymphoid cells (ILC2) is NOD2 dependent

Authors:

C. S. Hardman[1], Y. L. Chen[1], M. Salimi[1], J. Nahler[1], D. Corridoni[1], M. Jagielowicz[1], C.L. Fonseka[1], D. Johnson[2], E. Repapi[3], D. J. Cousins[4,5], J. L. Barlow[6], A. N. J. McKenzie[6], A. Simmons[1], G. Ogg[1*].

Affiliations:

[1]MRC Human Immunology Unit, NIHR Biomedical Research Centre, Radcliffe Department of Medicine, University of Oxford, UK

[2]Department of Plastic and Reconstructive Surgery, John Radcliffe Hospital, Oxford University Hospitals NHS Trust, UK

[3]CBRG, MRC Weatherall Institute of Molecular Medicine, Oxford, UK

[4]Department of Infection, Immunity and Inflammation, NIHR Leicester Respiratory Biomedical Research Unit, University of Leicester, UK

[5]MRC & Asthma UK Centre in Allergic Mechanisms of Asthma, King's College London, UK

[6]MRC Laboratory of Molecular Biology, Cambridge, UK

* Corresponding author

One sentence summary

Human ILC2 express NOD2 and secrete IL-6 in response to bacterial ligands.

Abstract

Cutaneous group 2 innate lymphoid cells (ILC2) are spatially and epigenetically poised to respond to barrier compromise and associated immunological threats. ILC2, lacking rearranged antigen-specific receptors, are primarily activated by damage-associated cytokines and respond with type-2 cytokine production.

To investigate ILC2 potential for direct sensing of skin pathogens and allergens we perform RNA-sequencing of ILC2 derived from *in vivo* challenged human skin or blood. We detect expression of *NOD2* and *TLR2* by skin and blood ILC2. Stimulation of ILC2 with TLR2-agonist alone induces IL-5 and IL-13 expression, but in combination with *Staphylococcus aureus* muramyl dipeptide (MDP) elicits IL-6 expression. Heat-killed skin-resident bacteria provoke an IL-6 profile in ILC2 *in vitro* that is strikingly impaired in ILC2 derived from patients with *NOD2* mutations. In addition, we show NOD2 signaling stimulates autophagy in ILC2 which is also impaired in patients with *NOD2* mutations. Here through identification of ILC2 NOD2 signaling we highlight the differential regulation of ILC2-derived IL-6, and report a previously unrecognized pathway of direct ILC2 bacterial sensing.

Introduction

Innate lymphoid cells (ILC) have typical lymphocyte morphology, originate from the common lymphoid progenitor (*1*) and mirror the T-helper subsets in transcription factor dependence and cytokine production. Human ILC2 have been identified in the blood, skin, nasal, gut and lung tissue (*2*). ILC2 constitute approximately 0.1% of blood lymphocytes, but are principally tissue-resident professional cytokine-producing cells, enriched in number and functional potential in barrier and mucosal tissues (*3*). Unlike T cells, ILC lack antigen-specific rearranged receptors and are thought to be primarily activated by innate alarmin-like signals. ILC2 are identifiable by a lack of certain cell surface markers for known lineages and are positively defined by IL-7Rα and CRTH2 expression (*4*). CRTH2 is the receptor for the lipid mediator and ILC2-activating factor PGD_2, which is released primarily from activated/degranulating mast cells during infection and allergy (*5*). ILC2 are also characterized by cell surface expression of the receptors for the alarmin cytokines IL-25, IL-33 and TSLP (*6*). Indeed, ILC2 type-2 cytokine production is thought to be predominantly activated by these type-2 inducer cytokines and inflammatory lipid mediators such as PGD_2 and LTE_4. IL-33, is amongst the most potent of the ILC2 inducer-cytokines (*6*), and is released passively from the nucleus of epithelial cells upon necrosis; however there is evidence that IL-33 is produced by a number of hematopoietic cells and other non-hematopoietic cells. Analysis of human skin biopsies and murine studies have established that skin trauma induces IL-33-dependent ILC2 proliferation, migration and production of epithelial growth factor amphiregulin (*7-9*). Notably, abrogation of these ILC2 responses impaired efficient wound closure. Amphiregulin has also been shown to be important in the ILC2 response to influenza in the lung (*10*). In addition to passive release upon epithelial damage, type-2 inducer cytokines and skin-specific ILC2-activating cytokines (e.g. IL-18) are produced by keratinocytes following TLR

sensing of atopic dermatitis (AD) skin-colonizing *S. aureus* (*11*). ILC2-derived IL-13 and IL-5 have been shown to be crucial for protective responses to *Nippostrongylous brassiliensis* (*12*) and pathogenic in the development of allergic asthma (*13*) and AD-like lesions (*8*). Additionally, it is increasingly understood that ILC2 can produce an array of non-classical type-2 cytokines including GM-CSF and IL-8 through which ILC2 can orchestrate innate and adaptive immune responses (*5*).

ILC2 are the predominant ILC population within the skin. Cutaneous ILC2 are spatially and epigenetically poised to respond to barrier compromise and associated immunological threats. In contrast, $CD4^+$ T cells must undergo significant chromatin remodeling on activation, highlighting the unique position of ILC2 as sentinels and early effectors mediating responses to cutaneous and mucosal barrier breach (*14*). As well as being resident in healthy human skin, we and others previously showed that ILC2 are increased in abundance and are activated within AD lesional skin (*8, 9, 15*). Notably ILC2 in AD lesions display elevated IL-25R, IL-33R and TSLPR levels. In murine models of dermatitis (*8, 16, 17*), ILC2 are increased in frequency and potently produce IL-4, IL-5 and IL-13, key effectors of AD immunopathology (*15, 18*). ILC2 dysregulation in AD may in part be mediated by loss of E-cadherin-KLRG1 dependent inhibition of cutaneous ILC2 (*8*), possibly due to filaggrin deficiency (*19*).

In addition to sensing the microenvironment via the cytokine/proinflammatory milieu there is increasing evidence ILC2 can be activated by a diverse range of direct innate signals. Cutaneous $NKp30^+$ILC2 sense increased expression of B7H6 in AD lesions and tumors, inducing type-2 cytokine production (*9*). ILC are reported to express a variety of TLRs (*20-22*), however the resulting effector cytokine production may in part depend on cytokine costimulus (*23*). We have previously shown that ILC2 TLR2 and TLR4 signaling not only induces cytokine production, but

can induce PLA2G4A phospholipase activity, which was suggested to contribute to ILC2 antigen presentation in the skin (*24*). Human cutaneous ILC2 have been shown to express the antigen presentation molecules MHCII and CD1a (*24*, *25*) which facilitate dialogue with T cells. However, the exact nature of the role of ILC2 pattern recognition receptor (PRR) signaling is yet to be fully elucidated and may be important for interaction with commensal and pathogenic microflora of the skin. ILC interaction with the microbiome has been documented within skin follicles. Skin ILC-derived TNF and lymphotoxins act on sebaceous glands to regulate production of sebum anti-microbial palmitoleic acid and bacterial commensals (*26*).

NOD2 is an intracellular PRR (*27*) which senses bacterial peptidoglycan motifs in the cytosol, the most basic of which, common to gram-positive and negative bacteria, is MDP. After recognition of MDP, NOD2 activates MAPK (*28*) and NF-κB (*29*) via well-characterized pathways leading to inflammatory and antimicrobial responses. NOD2 plays a key role in host defense through the recognition of pathogenic bacteria and ssRNA viruses (*30*), induction of autophagy (*31*), and homeostasis with commensal bacteria (*32*). In this study we use a human skin challenge model to investigate the role of pattern recognition signaling to induce ILC2 cytokine production, with findings that show a previously unappreciated mechanism for ILC2 in cutaneous bacterial surveillance.

Results

Human blood and skin ILC2 can express NOD2

ILC2 have been shown to regulate cutaneous barrier protection through orchestration of wound re-epithelialization (*7*) and allergic immunity in response to innocuous allergens of the skin (*8*). To analyze the phenotype of cutaneous ILC2 upon *in vivo* human allergic challenge, skin suction blisters were formed after intradermal injection of house dust mite (HDM) allergen on the arm of a healthy HDM-sensitive index participant. Twenty-four hours later, ILC2 were isolated by fluorescence guided cell sorting and gene expression analyzed by RNA sequencing (*24*) (fig. S1A). The main advantage of the skin suction blister model is that cells are isolated directly from the skin without the need for enzymatic processing, which risks exogenous modulation of gene expression. T cells and blood-derived ILC2 were isolated and analyzed in parallel, to aid identification of specific ILC2 gene expression. To assess the capacity for ILC2 to sense the cutaneous microenvironment we analyzed our RNA-seq data set for PRR expression. We found that blister and blood ILC2 express a broad range of PRRs (Fig. 1A). Indeed, *TLR2* was highly expressed by blister infiltrating ILC2, as we reported previously (*24*). We were surprised to detect that both skin and blood ILC2 expressed the gene encoding intracellular PRR NOD2. Indeed, on further analysis of the dataset we found a number of NOD2-signaling associated genes expressed by both skin-infiltrating and blood ILC2 (Fig. 1B). We went on to validate the RNA-seq skin suction blister result in multiple donors and under steady state conditions. We isolated human blood ILC2 to confirm the expression of *NOD2* by real-time PCR, and found that *NOD2* could be upregulated by ILC2 stimulation with IL-33 (Fig. 1C). ILC2 *NOD2* expression was significantly greater than observed in T cells (and not induced by stimulation of T cells with IL-33 or PMA/ionomycin), as suggested in the RNA-seq dataset. Further, we confirmed the expression of

NOD2 protein by human ILC2 using flow cytometry, in both blood and skin biopsy samples (Fig. 1D-F and fig. S2A. NOD2 expression was assessed in blood and skin ILC2 *ex vivo* and cultured blood-derived ILC2 (fig. S2A). NOD2 was found to be most highly expressed within skin ILC2 (Fig. 1E and fig. S2A), additionally the expansion and culturing process did not significantly alter blood ILC2 NOD2 expression. It is of interest that $NOD2^+$ ILC2 were enriched in the skin where ligand exposure would be most likely. This prompted investigation of the cutaneous localization of $NOD2^+$ ILC2 within the skin. Skin biopsies were subjected to dispase treatment to separate epidermis and dermis, which were both then enzymatically digested to allow determination of $NOD2^+$ ILC2 frequency within the compartments. We found enrichment of $NOD2^+$ ILC2 within the epidermis at the forefront of the barrier (Fig. 1F). Human blood and skin samples were additionally analyzed *ex vivo* for NOD2 expression by ILC subsets. We found NOD2 expression in all three subsets, however expression was highest in ILC2. We therefore focused this study on ILC2 as the predominant ILC population in the skin and key pathway of atopic dermatitis inflammation (fig. S2B). ILC2 NOD2 protein cellular expression was enhanced by stimulation with IL-33 and PGD_2 (Fig. 1G), in human blood ILC2 that had been isolated by flow cytometry (fig. S1B-C) and expanded *in vitro* for use in functional experiments. PGD_2 and IL-33 were used in combination to attempt maximal stimulation of ILC2, with IL-33 being the most potent cytokine activator of ILC2 and PGD_2 receptor, $CRTH_2$, being the population defining marker for isolation of human ILC2. With these observations we report for the first time the presence of PRR NOD2 within ILC2.

ILC2 are capable of NOD2 pattern recognition receptor signaling

To further investigate potential for ILC2 NOD2 signaling we explored the uptake of MDP by ILC2. Analysis of our RNA-Seq dataset for known MDP transporters revealed blood and blister ILC2 expression of *SLC15A3* and *SLC15A4* suggesting the capacity for MDP to be taken up by endocytosis (*33-35*) (Fig. 2A). Human blood ILC2 were isolated, expanded and cultured with fluorescent MDP or unconjugated Rhodamine B control (MDP-Rhodamine, 5µg/ml for 3 hours) and uptake visualized by flow cytometry (Fig. 2B and fig. S1D) and confocal microscopy (Fig. 2C and fig. S3). ILC2 were stimulated 1 hour prior to addition of MDP-Rhodamine and we found that TLR2 signaling could increase MDP uptake which may add to our understanding of the published synergistic function of MDP and Pam_3CSK_4 (*36*). To determine the functional significance of ILC2 PRR expression highlighted here, we isolated and expanded ILC2 from human blood and stimulated with a panel of PRR (TLR and NLR) ligands/agonists. TLR2 (agonist: Pam_3CSK_4) and TLR4 (agonist: LPS) stimulation elicited strong cytokine responses, inducing *IL-13* and *IL-5* upregulation. Interestingly the same PRR signals induced IL-6 production, a cytokine that is less well understood in ILC2-mediated biology. Strikingly, amongst the cytokines analyzed, *IL-6* only was upregulated by MDP stimulation of NOD2 (Fig. 2D). These data suggest ILC2 are capable of functional PRR responses, notably NOD2 signaling.

NOD2 signaling induces IL-6 effector cytokine production

NOD2 often acts in concert with other PRRs, in particular TLR2 (*36-38*). NOD2 and TLR2 both recognize conserved components of the peptidoglycan (PGN) found in bacterial cell walls and are thought to act synergistically. NOD2 stimulation alone typically results in weak responses yet is greatly enhanced by concomitant TLR2 signaling, thought to upregulate *NOD2* gene expression (*39*). Since expression of TLR2 was highly detected on ILC2, we assessed the effect of NOD2

costimulation with Pam_3CSK_4 on ILC2 cytokine expression. We observed that whilst Pam_3CSK_4 stimulation increased *IL-13* and *IL-5* gene expression, MDP with Pam_3CSK_4 had the most profound effect on *IL-6* expression (Fig. S4A). We assessed the effect of TLR2 stimulation on *NOD2* gene expression and found that combinations of Pam_3CSK_4 and MDP induced upregulation of *NOD2* expression (Fig. S4B and Fig. 3A). This finding is also interesting given our observation that Pam_3CSK_4 could increase MDP uptake by ILC2. Following MDP sensing, NOD2 recruits RIPK2 via CARD domain interaction. Given the importance of RIPK2 in the NOD2 signaling pathway, we next sought to determine the effect of ponatinib, a specific RIPK2 inhibitor that functions by blocking RIPK2 autophosphorylation and ubiquitination, on ILC2 stimulation. We found that ponatinib ablated the stimulatory effect of MDP/ Pam_3CSK_4 on ILC2-derived IL-6 but not IL-13, suggesting the primary stimulatory factor inducing IL-13 was Pam_3CSK_4 (Fig. 3A). Furthermore, in addition to IL-6 production we assessed the capacity for NOD2 signaling to induce the production of ILC2-derived IL-8, and found that this was significantly inhibited by ponatinib (Fig. 3A). IL-8 is a well-defined effector cytokine of NOD2 signaling, important for protective neutrophilia induced during bacterial infection (*40*).

Classical cytokine activation of ILC2, by IL-33 or PGD_2, induced IL-13 and IL-5, and IL-8 production but did not affect ILC2 production of IL-6 (Fig. 3B). To assess a possible role for ILC2 PRR signaling as a costimulus to classical cytokine/alarmin signaling, which could direct or bias the effector cytokine response, we stimulated human blood-derived ILC2 with IL-33, PGD_2, MDP and/or Pam_3CSK_4. Elevated IL-6 expression and secretion were detected by RT-PCR after 6 hours and ELISA analysis of culture supernatant after 5 days of IL-33 and MDP/ Pam_3CSK_4 costimulation (Fig. 3C-D).

To confirm NOD2-induced IL-6 production was not an artefact of *in vitro* cultured ILC2, we performed stimulation of blood and skin-biopsy mononuclear cells *ex vivo,* without population isolation and expansion, and assessed the response of ILC2 by flow cytometry. *Ex vivo* blood and skin ILC2 produced IL-6 and IL-8 in response to MDP/ Pam_3CSK_4 and IL-13 in response to IL-33 and PGD_2 (Fig. 3E). With *in vitro* isolated and cultured blood ILC2 we confirmed NOD2-dependent production of IL-6 resulting from MDP/ Pam_3CSK_4 stimulation which was lost upon prior incubation with ponatinib (Fig. 3F). In contrast, although IL-13 production was induced by MDP/ Pam_3CSK_4, it was not significantly reduced by ponatinib suggesting Pam_3CSK_4 rather than MDP was the main stimulatory factor (Fig. 3F). IL-6 is a well-established product of NOD2/TLR2 signaling for macrophages and mononuclear cells (*36, 39*), here we report NOD2 selective induction of ILC2-derived IL-6.

ILC2 are capable of sensing skin-resident bacteria via NOD2 inducing IL-6 production

TLR2, TLR4 and NOD2 are important components of the recognition of PAMPs/pathogens. We sought to determine the role of ILC2 PRR signaling in bacterial surveillance. Commensal bacteria constitute part of a healthy skin barrier which is dysregulated in disease, for example an increased density of *S. aureus* is associated with at least 70% of AD cases (*41*). We used heat-killed bacterial preparations of skin-associated bacteria to assess the potential for ILC2 sensing of the cutaneous microbiota including *S. aureus, S. epidermidis* and *Pseudomonas aeruginosa*. *S. aureus* (SA) is associated with skin infections, AD, and more serious systemic infections and non-healing wounds. *S. epidermidis* (SE) is a benign commensal in most instances but seen as an opportunistic pathogen. *P. aeruginosa* (PA) an opportunistic pathogen sometimes colonizing burns and surgical wounds. We observed IL-6, but not IL-13, production upon stimulation of purified ILC2 with

bacterial preparations of *S. aureus* and *S. epidermidis*, which was significantly reduced by inhibition of NOD2 signaling with ponatinib. A similar but non-significant trend was observed for *P. aeruginosa* (Fig. 4A). Furthermore IL-8 production appeared to show a similar trend to the IL-6 response. Analysis of blood (Fig. 4B) and skin-biopsy (Fig. 4C) ILC2 stimulated *ex vivo*, within the mononuclear cell population, with heat-killed bacteria revealed a similar bias in ILC2 effector cytokine production. Skin-associated heat-killed bacteria induced IL-6 and IL-8 but not IL-13 (Fig. 4A-C). Interestingly, concurrent staining of ILC2 cytokine production revealed almost mutually exclusive expression of IL-6 and IL-13 upon bacterial preparation stimulation (fig. S5A-B). With *in vitro* cultured purified ILC2, we confirmed NOD2-dependent production of IL-6 protein upon bacterial stimulation, which was lost upon prior incubation with ponatinib (Fig. 4D). In contrast, although IL-13 production may be induced by bacterial preparations, it was not significantly reduced by ponatinib suggesting a NOD2-independent main stimulatory factor (Fig. 4D). In summary these results suggest ILC2 may utilize NOD2 signaling to sense skin resident bacteria and induce an altered cytokine response with implications for allergic disease and wound healing.

ILC2 IL-6 effector response to bacterial components is ablated in patients with NOD2 mutations

NOD2 signaling is associated with inflammatory disorders, including being the strongest associated IBD susceptibility gene. Notably, the *NOD2* polymorphism R702W has also been associated with AD (*42*). We sought to determine whether NOD2 signaling defects reduced the ILC2 capacity to sense skin-colonizing bacteria. We stimulated PBMC derived from patients with *NOD2* loss of function homozygous mutations with heat-killed bacterial preparations as well as bacterial components Pam_3CSK_4 and MDP and assessed effector cytokine production by flow

cytometry compared to healthy donors with wild-type *NOD2*. We found IL-6 production was diminished in ILC2 derived from patients with *NOD2* mutations, as compared to wild-type healthy control samples. In healthy donors MDP, Pam_3CSK_4 and heat-killed bacteria induced IL-6 production. Strikingly in patients with *NOD2* mutations, the IL-6 response was ablated (Fig. 5A and fig. S5C). In contrast, the IL-13 production was unaffected by *NOD2* mutation status (Fig. 5B and Fig. S5C). Interestingly, skin homing marker CLA was upregulated by blood ILC2 stimulated within the PBMC population upon NOD2 stimulation and IL-33 and PGD_2. This increase in CLA expression was lost upon NOD2 stimulation of circulating ILC2 derived from patients with *NOD2* mutations (fig. S6A). To further investigate the clinical relevance of these findings to cutaneous expression of NOD2, we genotyped our small cohort of AD patients for *NOD2* SNPs. We observed the AD-associated R702W mutation at a high frequency, heterozygous in three AD patients (of eleven genotyped) and zero healthy volunteers (of seven genotyped) (fig. S6B-C); these data confirm the findings of *Macaluso et. al.* (*42*). *NOD2* mutations are not present in all AD patients, and so we investigated the effector cytokine response of ILC2 derived from wild-type-*NOD2* AD patients. ILC2 were analyzed *ex vivo* within the PBMC population (Fig. 6A-B) and following isolation, expansion and culture (Fig. 6C). We saw that wild-type *NOD2* AD ILC2 were more responsive to NOD2 signaling and produced IL-6 at a higher basal level (Fig. 6C). Additionally, AD ILC2 produced IL-13 at a higher basal level *ex vivo*, suggestive of a highly proinflammatory state. Of note ILC2 derived from patients with the R702W heterozygous mutation responded to NOD2 stimuli with significantly less IL-6 than wild-type-*NOD2* AD ILC2 (fig. S6D). Furthermore, NOD2 was found to be expressed at a higher level by AD patient than healthy volunteer blood-derived ILC2 (Fig. 6D). Analysis of ILC2 derived from patients with

NOD2 mutations and AD has informed our understanding of NOD2 induced cytokine bias in ILC2 with potential implications for AD immunopathology.

NOD2 stimulation can induce ILC2 autophagy

Autophagy is a crucial mechanism of bacterial immunity and conversely can be co-opted by certain bacteria to infiltrate host cells. In addition to cytokine production, NOD2 signaling induces autophagy as a bacterial defense mechanism. Autophagy is important for skin homeostatic and inflammatory processes, including *S. epidermidis* and *S. aureus* immunity. Our ILC2 RNA-seq data set revealed expression of a number of autophagy-associated genes in blood and blister-infiltrating ILC2 (fig. S7). We detected expression of ATGL16 the NOD2 binding protein which is crucial for assembly of the autophagic complex (fig. S7).

To investigate the role of autophagy in ILC2 bacterial sensing, we analyzed autophagic potential of ILC2 *ex vivo* in human PBMC and skin-biopsy derived mononuclear cells following stimulation with heat-killed bacterial preparations and PRR agonists. Using LC3-II as a surrogate for autophagy measured by flow cytometry, we observed TLR2 and NOD2 ligands induced autophagy in skin ILC2. A similar trend was observed for blood ILC2 although significance was not reached. The most striking induction of autophagy in ILC2 was seen in response to heat-killed *S. aureus* and *S. epidermidis* (Fig. 7A-B). To confirm ILC2 intrinsic induction of autophagy by bacterial preparations/PAMPs, we purified ILC2 from human blood, expanded the cells *in vitro* and stimulated them with NOD2 agonists, heat-killed skin bacteria or IL-33. We observed induction of LC3-II^{+} autophagosomes by flow cytometry upon NOD2 and bacterial stimulation (Fig. 7C and fig. S8), suggesting ILC2 are capable of sensing bacteria and enacting an autophagic response. Autophagosome formation was assessed in ILC2 derived from patients with *NOD2* mutations; LC3-II induction was ablated (Fig. 7D). Given the importance of autophagy for ILC2 modulation

of metabolic fuel usage and as such effector cytokine responses (*43*), we set out to investigate the potential functional consequences of NOD2 induced ILC2 autophagy. Using ILC2 purified and expanded from healthy volunteers, we inhibited autophagy using 3-Methyladenine (3MA, 5mM, 1 hour) and then stimulated ILC2 with NOD2 ligand sources for 10 hours, we then added IL-33 and PGD_2 to the culture system to induce a robust type-2 cytokine response (50ng/ml and 100nM overnight, respectively). We assessed ILC2 IL-13 production by intracellular flow cytometry and found a NOD2-dependent increase in IL-33/PGD_2-induced IL-13 production, which was lost on autophagy inhibition. These data suggest that ILC2 intrinsic NOD2 signaling can influence the type-2 cytokine response in addition to directly inducing IL-6 production independent of type-2 inducer cytokines (Fig. 7E).

Taken together these data define a previously unappreciated role for ILC2 in the sensing of skin resident bacteria through NOD2 with resulting IL-6 effector cytokine bias and autophagic potential.

Discussion

NOD2 is expressed in the intestine by numerous cell types, including hematopoietic cells (*44*) (B cells (*45*), macrophages (*46, 47*), dendritic cells (*48*), mast cells (*49*), monocytes (*50*), eosinophils (*51*), and neutrophils (*52*)) and non-hematopoietic cells (Paneth cells (*53*), stem cells (*54*), goblet cells (*55*), and enterocytes (*56, 57*)). Within the skin, NOD2 expression is less well characterized but has been reported in keratinocytes (*58, 59*). Here we report the previously unrecognized expression of functional NOD2 in human ILC2. NOD2 was expressed by both circulating and cutaneous skin-infiltrating ILC2. In addition to NOD2 we detected gene expression of a number of NOD2 binding partners, some of which interact directly with NOD2 to enhance or inhibit functional activity (*60*). Interestingly, we noted expression of genes encoding the following negative regulators of NOD2 signaling Erbin, Centaurin B1, Angio-Associated Migratory Cell Protein, Carbamoyl-Phosphate Synthetase 2, Mitogen-Activated Protein Kinase Binding Protein 1 (JNKBP1) and Suppressor of Cytokine Signaling-3 (*60-64*) in blood and skin ILC2. Careful regulation of NOD2 signaling would be required in the skin, where an effective dialogue between immune cells and the microbiome is key for a heathy barrier. Indeed, uncontrolled NOD2 signaling could lead to a highly proinflammatory state in the skin and dysbiosis. Furthermore, we found evidence that IL-33 and PGD_2 could amplify the NOD2 response in ILC2 possibly through increase of NOD2 expression. Thus, the cytokine microenvironment can skew the resulting NOD2 immune cascade with potential NOD2 signaling regulation mechanisms governing ILC2-intrinsic responses.

Our findings add to the understanding of ILC2 effector cytokine regulation; we show that whereas alarmin cytokine activation of ILC2 induces IL-13 and IL-5, combined NOD2 and TLR2 signaling biases ILC2 cytokine production towards IL-6 and IL-8. Through direct sensing of PAMPs (MDP

and Pam_3CSK_4), as opposed to DAMP/alarmin cytokines (IL-33/PGD_2), ILC2 induced an altered cytokine profile dominated by IL-6 and IL-8. These discrete cytokine-producing ILC2 could represent distinct populations of ILC2, or an activation state induced by microenvironmental cues. *NOD2*$^{-/-}$ mice are reported to have a delayed and damaging response to *S. aureus* with increased skin lesions and impaired bacterial clearance, which is dependent on IL-6 (*58*). Similarly, in a sterile wound setting *NOD2* deficiency leads to a substantial defect in wound repair associated with an initial delay in neutrophil recruitment (*65*). Additionally, *IL-6*$^{-/-}$ mice have greatly increased skin inflammation following chemical irritant challenge, showing that NOD2 and IL-6 are important for efficient wound healing and response resolution. When the skin barrier is compromised, bacteria can colonize the wound and impair healing and contribute to the inflammation of skin lesions in AD. *NOD2* deficiency results in increased bacterial abundance following injury and delays wound closure. Interestingly *NOD2*$^{-/-}$ mouse wounds are reportedly colonized by the opportunistic pathogenic species *P. aeruginosa* and this was linked to chronic inflammation and wound infection (*66-68*). There is evidence that NOD2 modulates both proinflammatory and anti-inflammatory effects depending on the presence of cytokines or bacterial products in the microenvironment (*69*). Therefore, more information is required to understand the role of NOD2 in wound healing.

ILC interaction with the microbiome has been reported within skin follicles regulating bacterial commensalism (*26*). Here we show that ILC2 can detect *S. aureus, S. epidermidis* and *P. aeruginosa* via NOD2 and induce differential ILC2 cytokine production, IL-6 and IL-8, and we suggest a further pathway in which ILC2 may play an important role in regulating the skin microflora and maintaining homeostasis and wound healing capacity. *S. aureus*, a clinically important pathogen that causes skin infection in patients with AD, has been previously

demonstrated to induce autophagy (28). NOD2 recruits ATG16L1 to the plasma membrane at the site of bacterial entry for the encapsulation of the invading bacterium in an autophagosome (*31*). This pathway was lost in cells homozygous for Crohn's disease (CD)-associated *NOD2* loss of function mutation resulting in increased intestinal inflammation and bacterial load (*70-72*). Notably, *ATG16L1* and *NOD2* SNPs are both implicated in increased susceptibility to CD (*70*, *73-75*). More recently, additional RIPK2-dependent mechanisms of NOD2-dependent autophagy induction have been proposed in DCs (*48*) and macrophages, where TLR2 and NOD2/RIPK2 deficiencies lead to defective autophagic responses to *Listeria monocytogenes* (*76*).

Here we found NOD2 agonists and heat-killed bacterial preparations induced formation of LC3-II^+ autophagosomes in a NOD2-dependent manner in ILC2. We observed that autophagy was induced by cytokines, IL-33 and PGD_2, and NOD2 signaling. Mutations in autophagy related genes, including *NOD2* and *NLRP12*, have been associated with AD. Autophagy contributes to the maintenance of the cutaneous barrier, inflammation, defense against invading pathogens (*S. aureus*) and keratinocyte homeostasis (*77*). We observed loss of MDP/Pam_3CSK_4-induced amplification of IL-33 and PGD_2-induced IL-13 production upon inhibition of autophagy (*43*). Furthermore, patients with NOD2 loss of function SNPs may lack protective anti-microbial ILC2-derived IL-6 and IL-8 signaling thus exacerbating AD, as suggested by our results showing greater NOD2 expression and IL-6 production in wild-type-*NOD2* AD patient ILC2.

Polymorphisms in the gene encoding NOD2 are associated with chronic inflammatory diseases, including CD (*78*), inflammatory skin disease Blau Syndrome (*79*) and early onset sarcoidosis (*80*). The three main *NOD2* polymorphisms, R702W (*42*), G908R and L1007fsinsC, are highly associated with susceptibility to CD; indeed *NOD2* is the strongest susceptibility gene for IBD (*78, 81, 82*). These mutations result in NOD2 loss of function, reduced responsiveness to MDP, which

enables invasion of bacteria and abnormal mucosal immunity, culminating in chronic intestinal inflammation (*78, 81, 83, 84*). Moreover, due to the dysbiosis *NOD2*$^{-/-}$ mice display increased sensitivity to dextran sulfate sodium-induced colitis and colonic adenocarcinoma (*85, 86*). *NOD2* polymorphisms, particularly R702W, have also been linked to AD, indeed we found heterozygous mutations in our AD cohort; importantly AD is characterised by exacerbation of *S. aureus*-related inflammation (*42, 87, 88*). *S. aureus* infection of human keratinocytes induces *NOD2* gene expression and consequently IL-17C production. Furthermore the S. *aureus* load was significantly reduced in keratinocytes overexpressing functional NOD2 (*89*).

In this study we found that NOD2 mutation/blockade significantly reduced ILC2-derived IL-6 and autophagic responses to heat-killed skin bacterial preparations. These data however, may have implications for atopic dermatitis patients with *NOD2* mutations, suggesting a further ILC2-dependent mechanism by which NOD2 mutation can impact on AD immunopathology through altered cytokine production and autophagy. Indeed here we highlight the heterogeneity of AD immunopathology where three patients of our AD cohort (n=11) displayed heterozygous R702W mutations which appeared to result in reduced ILC2 IL-6 production potential in response to NOD2 stimulation, which we suggest may contribute to reduction in anti-microbial and pro-wound healing effects of the NOD2 pathway characteristic of AD lesions. Conversely in the wild-type-*NOD2* group of AD patients, increased IL-6 production potential was observed with an increase in NOD2 expression, this may contribute to the published increase in IL-6 in AD patients (*90, 91*) and exacerbate the proinflammatory effects of NOD2/IL-6 and IL-13 signaling resulting in damaging inflammation in the skin.

Elucidation of the roles of cutaneous ILC2 has provided us with new targets for therapeutic intervention. ILC2 are not unique in expression of NOD2 in the skin, other more abundant cells play important roles in the NOD2 pathway, however we envisage ILC2 occupying a unique niche in the NOD2 response, combining antigen sensing power via NOD2, TLR2, MHCII and CD1a, with rapid cytokine production that orchestrates the ensuing immune response. Activation of ILC2 via NOD2 has the potential not only to orchestrate the immune response by IL-6 production but to influence other NOD2 expressing cell populations and tailor the ensuing anti-bacterial and allergic immune response.

Materials and methods

Study design

The study was designed to test the hypothesis that ILC2 can sense bacterial ligands/PAMPs via NOD2 and TLR2. Adult participants were only excluded if on systemic immunosuppression or topical calcineurin inhibitors. Clinic participants were recruited sequentially; blinding and randomization were not required as there was no intervention. All study participants gave fully informed written consent. Thus variation between the functional responses of different donors is expected as cells were isolated from individuals of differing, age, gender, ethnicity and medical history, although broadly defined as healthy controls. The nature of functional human ILC2 experiments requires the expansion of primary ILC2. We use flow cytometry to sort ILC2 at 100 cells per well and expand the cells using MLR, as detailed below, as such ILC2 lines could have variable receptor expression and therefore functional responses over and above inter-donor variation. Sample size was determined based on previous studies of ILC2 responses in humans (*8*, *9*, *24*). All experiments were replicated as presented in the figure legends.

Antibodies and flow cytometry

For FACS surface staining the cells were labelled with the following anti-human antibodies: CD3 (OKT3, Biolegend, BV650 : 317324), CD19 (HIB19, Biolegend, PerCP : 302228), CD123 (32703, Bio-Techne, PerCP : FAB301C), CD11b (M1/70, Biolegend, PerCP : 101230), CD11c (BU15, Biolegend, PerCP : 337234), CD8 (RPA-T8, Biolegend, PerCP : 301030), FcεRI (CRA-1, Biolegend, PerCP : 334616), CD14 (HCD14, Biolegend, PerCP : 325632), CD4 (OKT4, Biolegend, PerCP : 317432), CD45 (2D1, Biolegend, AF700 : 368514), CD56 (HCD56,

Biolegend, BV605 : 318334, PerCP : 318342), CRTH2 (BM16, Miltenyi Biotec, PE : 130-113-600), IL-7Ra (A019D5, Biolegend, PECy7 : 351320), Live/Dead violet or Aqua (Invitrogen). Intracellular cytokine staining was completed using the eBioscience FoxP3 Fix/Perm kit as per the manufacturer's instructions with 10 hour Brefeldin-A (eBioscience) treatment and stained with anti-IL-13 (85BRD, Life Technologies, FITC : 11-7136-42), IL-6 (MQ2-13A5 Biolegend, APC : 501112), IL-8 (E8-N1, Biolegend, APC : 511410), NOD2 (2D9 : Bio-Techne, NB100-524), LC3b (ab51520, abcam) antibodies.

Suction blister technique

Suction blister cups were applied to the skin of the forearm of a healthy adult volunteer with sensitivity to house dust mite (HDM) allergen under local ethics approval (National Research Ethics Service Committee South Central, Oxford C, 09/ H0606/71), at a vacuum pressure of 250 mmHg. Blisters were generated over the site of a HDM intradermal injection. Blisters were formed within 30 – 90 min of suction application. Blister fluid was aspirated 24 hours later using a 30 gauge needle. Fluids were then centrifuged at 1500 rpm for 5 min at 4°C and the cells were stained with cell surface antibodies for flow cytometric isolation of ILC2 and T cells utilized for RNA Sequencing analysis (*24*). This experiment was performed in one index donor. However, to validate the RNA-seq skin suction blister result in multiple donors and under steady state conditions, samples of healthy unchallenged human skin were analysed *ex vivo* for expression of NOD2 by ILC2 using flow cytometry.

RNA Sequencing

Suction blister fluid and blood derived PBMCs were centrifuged at 1500 rpm for 5 minutes at 4°C to pellet the blister-infiltrating cells, which were re-suspended in PBS. Blister and blood cell populations were isolated by flow cytometry and collected directly into TRIzol LS; T cells ($CD3^+$ $CRTH2^+$) and ILC2 (Lin^- $CD45^+$ $CD3^-$ IL-7Rα^+ $CRTH2^+$). The manufacturer's protocol was followed for TRIzol LS mRNA extraction as far as "Phase Separation". The RNA containing phase was then processed using Qiagen RNAeasy mini kit and contaminating DNA was removed using Ambion Turbo DNase. The total purified RNA was then processed using a NuGEN Ovation RNA-seq system V2 (Ultralow DR multiplex kit). Samples were sequenced on an Illumina HiSeq 2000. Following QC analysis with the fastQC package (http://www.bioinformatics.babraham.ac.uk/projects/fastqc), reads were aligned using STAR (63) against the human genome assembly (NCBI build37 (hg19) UCSC transcripts). Non-uniquely mapped reads and reads that were identified as PCR duplicates using Samtools (64) were discarded. Gene expression levels were quantified as read counts using the featureCounts function (65) from the Subread package (66) with default parameters. RPKM values were generated using the edgeR package (67).

Cell sorting and culture

PBMCs were isolated from healthy adult donors under local ethics approval (National Research Ethics Service Committee South Central, Oxford C, 09/ H0606/71). ILC2 were isolated and cultured as previously described (7). Briefly, the lineage (CD3, CD4, CD8, CD14, CD19, CD56, CD11c, CD11b, CD123, and FcεRI)$^-$, $CD45^+$, IL-7Rα^+, $CRTH2^+$ ILC2 population was sorted into 96-well plates at 100 cells per well and resuspended in MLR of gamma-irradiated PBMCs from three healthy volunteers ($2x10^6$ cells / ml) coupled with 100 IU / ml IL-2 and PHA. After 4 – 6

weeks the growing cells were tested by flow cytometry staining to ensure a pure population of lineage$^-$CRTH2$^+$IL-7Rα$^+$ ILC2 was obtained (fig. S1B-C).

Cytokines and TLR agonists

For stimulation studies ILC2 were incubated in culture with stimulants and/or inhibitors (see table 1.) for 6 - 120 hours at 37°C as noted in the figure legend. Cells were then centrifuged at 1500 rpm for 5 minutes at 4°C and supernatant saved for ELISA and cells used for RT-PCR analysis or flow cytometry.

Table 1. Reagents for stimulation of ILC2.

Reagent	**Target**	**Concentration**	**Source**
IL-33	ST2	50ng/ml	Biolegend
PGD_2	$CRTH_2$	100nM	Enzo Life Science
TSLP	TSLPR	50ng/ml	Biolegend
Pam_3CSK_4	TLR1/2	1µg/ml	Invivogen
LPS	TLR4	10ng/ml	Invivogen
MDP	NOD2	10µg/ml	Invivogen
HKLM	TLR2	10^8cells/ml	Invivogen
PolyIC HMW	TLR3	1µg/ml	Invivogen
PolyIC LMW	TLR3	1µg/ml	Invivogen
FLA	TLR5	1µg/ml	Invivogen
FSL	TLR6/2	1µg/ml	Invivogen
Imiquimod	TLR7	1µg/ml	Invivogen

ssRNA	TLR8/NOD2	1µg/ml	Invivogen
ODN	TLR9	5µM	Invivogen
Ponatinib	Inhibits NOD2/RIPK	25µM	Cayman Chemicals
HKSA	-	10^8cells/ml	Invivogen
HKSE	-	10^8cells/ml	Invivogen
HKPA	-	10^8cells/ml	Invivogen
MDP-rhodamine	NOD2	5µg/ml	Invivogen
Rhodamine-B	Control	5µg/ml	Sigma
3-Methyladenine	Inhibits autophagy	5mM	Invivogen

Quantitative RT-PCR

mRNA extraction was performed using a TurboCapture 96 mRNA kit (Qiagen, 72251) following the manufacturer's instructions. cDNA was prepared from the mRNA using M-MLV reverse transcriptase (Invitrogen). Taqman probes for *GAPDH* (Hs02786624_g1), *NOD2* (Hs01550753), *IL6* (Hs00174131), *IL13* (Hs001743790), *IL5* (Hs01548712*), IL8* (hs00174103) were used to analyze gene expression of ILC2 cultures on a QuantStudio7 Flex real time PCR machine.

Analysis of immune cells within human skin biopsies

To analyze $NOD2^+$ populations in the skin, samples of human skin were processed as follows. Samples were taken under GCP guidance with ethical approval of the NRES Committee South

Central. Subcutaneous fat was removed using scissors and residual fat cells were scraped from the underside of the skin and hairs from the upper side using a sharp scalpel. To analyze the cells of whole thickness skin samples, the explants were cut in to < 0.5mm pieces using scalpel and scissors in petri dishes and incubated in collagenase P (1 mg / ml Roche) containing media overnight at 37°C in the petri dish. After overnight digestion, the remaining tissue was homogenized with a Pasteur pipette and endonuclease deoxyribonuclease I (DNase I) 200 Kunitz unit/ml (Roche 10104159001) was added for 15 minutes at room temperature then passed through a 70 μm strainer (VWR) and washed with cold 10 mM EDTA solution. After centrifugation, the pellet was resuspended in cold RPMI and passed through a 40 μm strainer ready for further analyses. To isolate the epidermis 1 cm^2 sections of skin were placed epidermis down in a petri dish containing 5 U / ml dispase at 4°C overnight. The epidermal layer was then peeled from the dermis with forceps and chopped up and placed in an Eppendorf of 0.5 % Trypsin 0.02 % EDTA at 37°C for 15 minutes. The samples were homogenized with a Pasteur pipette and strained through a 40 μM filter and diluted and washed in FCS containing media. The separated dermis was processed as above for the whole thickness skin samples using a 2.5 hour collagenase P digestion. The single cell suspensions were then stained with cell surface marker antibodies for flow cytometry.

Fluorescent imaging

ILC2 were stimulated for 1 hour with Pam_3CSK_4 or IL-33 and PGD_2 as reported in the main text and figure. Then a 3 hour incubation with MDP-rhodamine (Invivogen, 5μg/ml) or Rhodamine B control (Sigma, 5μg/ml) was used for detection of ILC2 uptake of MDP. ILC2 were then washed three times with PBS and applied to slides with cytospin and stored at -20°C. Slides were fixed with 4% PFA for 10 minutes and washed twice in PBS, then mounted using antifade mounting

medium with DAPI (Vector Laboratories Ltd), coverslips were applied, and slides were refrigerated in the dark until analyzed by confocal microscopy (Zeiss LSM 780 Confocal Microscope-Inverted Microscope; 25x/0.8 Imm Korr DIC M27; room temperature; Axiocam camera; Zen software), and Fiji was used for image processing, DAPI and/or MDP-Rhodamine positive cells were counted manually using the ImageJ multipoint tool.

Genotyping of NOD2 mutations

Blood was collected from patients with Crohn's disease and healthy volunteers and genomic DNA extracted. NHS National Research Ethics Service (NRES) research ethics committee (REC) references for the study include 18/WM/0237; GI 16/YH/0247 and IBD 09/H1204/30. Atopic dermatitis patient and healthy volunteer samples were collected under local ethics approval at OUH NHS dermatology clinic (National Research Ethics Service Committee South Central, Oxford C, 14/SC/0106). Samples were subjected to physical homogenization (with 100 mg of 1.4-mm ceramic beads, 4,000 r.p.m.) or Qiagen lysis buffer, and DNA was isolated using an DNeasy Blood & Tissue Kit (Qiagen). gDNA was then used as the template for Taqman MGB biallelic discrimination assay to identify SNPs rs2066844 (R702W), rs2066845 (G908R), and rs2066847, a frame-shift mutation (1007fs). The genotyping assays for rs2066844 (AB ID: C_11717468_20) and rs2066845 (AB ID: C_11717466_20) were supplied by Applied Biosystems. The genotyping assay for rs2066847 was custom developed by Applied Biosystems and used forward primer, GTCCAATAACTGCATCACCTACCT; reverse primer, CAGACTTCCAGGATGGTGTCATTC) and fluorophore-labeled TaqMan MGB probes (VIC-labeled, CAGGCCCCTTGAAAG; FAM-labeled, CAGGCCCTTGAAAG). Reactions were performed according to the manufacturer's instructions. Briefly, 10 ng of genomic DNA was

mixed with 12.5ul of 2×TaqMan Universal PCR Master Mix (No AmpErase UNG) and 1.25ul of 20 × SNP Genotyping Assay, and PCR was carried out on a QuantStudio7 Flex real time PCR machine (ThermoFisher Scientific). Thermal cycling conditions were: 95° C for 10 min followed by 40 cycles of 95° C for 15 s (melting step) and 60° C for 60 s (anneal/extend step). Detection of fluorescent signal was performed according to the recommended protocols for the QuantStudio7 Flex real time PCR machine, and the results were analysed using the accompanying Sequence Detection System Software V.1.3.1 (Applied Biosystems).

Statistical analysis

The one and two-way ANOVA tests, paired and unpaired T-tests were performed using GraphPad Prism version 6.00 (GraphPad Software). Error bars represent standard deviation as indicated.

Supplementary materials

Figure S1. Isolation of Skin Blister ILC2

Figure S2. NOD2 expression analysis of innate lymphoid cells

Figure S3. Imaging of MDP-rhodamine uptake by activated ILC2

Figure S4. NOD2 and TLR2 stimulation of ILC2

Figure S5. Skin resident bacterial preparation stimulation of ILC2 gating strategies

Figure S6. ILC2 *NOD2* mutation analysis

Figure S7. Skin and blood ILC2 may be capable of autophagy

Figure S8. ILC2 LC3-II gating strategy

References

1. D. E. Cherrier, N. Serafini, J. P. Di Santo, Innate Lymphoid Cell Development: A T Cell Perspective. *Immunity* **48**, 1091-1103 (2018).
2. J. L. Barlow, A. N. McKenzie, Type-2 innate lymphoid cells in human allergic disease. *Curr Opin Allergy Clin Immunol* **14**, 397-403 (2014).
3. B. S. Kim, Innate lymphoid cells in the skin. *J Invest Dermatol* **135**, 673-678 (2015).
4. J. M. Mjosberg *et al.*, Human IL-25- and IL-33-responsive type 2 innate lymphoid cells are defined by expression of CRTH2 and CD161. *Nat Immunol* **12**, 1055-1062 (2011).
5. L. Xue *et al.*, Prostaglandin D2 activates group 2 innate lymphoid cells through chemoattractant receptor-homologous molecule expressed on TH2 cells. *J Allergy Clin Immunol* **133**, 1184-1194 (2014).
6. J. L. Barlow *et al.*, IL-33 is more potent than IL-25 in provoking IL-13-producing nuocytes (type 2 innate lymphoid cells) and airway contraction. *J Allergy Clin Immunol* **132**, 933-941 (2013).
7. G. D. Rak *et al.*, IL-33-Dependent Group 2 Innate Lymphoid Cells Promote Cutaneous Wound Healing. *J Invest Dermatol* **136**, 487-496 (2016).
8. M. Salimi *et al.*, A role for IL-25 and IL-33-driven type-2 innate lymphoid cells in atopic dermatitis. *J Exp Med* **210**, 2939-2950 (2013).
9. M. Salimi *et al.*, Group 2 Innate Lymphoid Cells Express Functional NKp30 Receptor Inducing Type 2 Cytokine Production. *J Immunol* **196**, 45-54 (2016).
10. L. A. Monticelli *et al.*, Innate lymphoid cells promote lung-tissue homeostasis after infection with influenza virus. *Nat Immunol* **12**, 1045-1054 (2011).
11. A. T. Vu *et al.*, Staphylococcus aureus membrane and diacylated lipopeptide induce thymic stromal lymphopoietin in keratinocytes through the Toll-like receptor 2-Toll-like receptor 6 pathway. *J Allergy Clin Immunol* **126**, 985-993, 993 e981-983 (2010).
12. D. R. Neill *et al.*, Nuocytes represent a new innate effector leukocyte that mediates type-2 immunity. *Nature* **464**, 1367-1370 (2010).
13. J. L. Barlow *et al.*, Innate IL-13-producing nuocytes arise during allergic lung inflammation and contribute to airways hyperreactivity. *J Allergy Clin Immunol* **129**, 191-198 e191-194 (2012).
14. H. Y. Shih *et al.*, Developmental Acquisition of Regulomes Underlies Innate Lymphoid Cell Functionality. *Cell* **165**, 1120-1133 (2016).
15. B. Roediger *et al.*, Cutaneous immunosurveillance and regulation of inflammation by group 2 innate lymphoid cells. *Nat Immunol* **14**, 564-573 (2013).
16. Y. Imai *et al.*, Skin-specific expression of IL-33 activates group 2 innate lymphoid cells and elicits atopic dermatitis-like inflammation in mice. *Proc Natl Acad Sci U S A* **110**, 13921-13926 (2013).
17. B. S. Kim *et al.*, Basophils promote innate lymphoid cell responses in inflamed skin. *J Immunol* **193**, 3717-3725 (2014).
18. B. S. Kim *et al.*, TSLP elicits IL-33-independent innate lymphoid cell responses to promote skin inflammation. *Sci Transl Med* **5**, 170ra116 (2013).
19. A. Trautmann *et al.*, The differential fate of cadherins during T-cell-induced keratinocyte apoptosis leads to spongiosis in eczematous dermatitis. *J Invest Dermatol* **117**, 927-934 (2001).
20. N. K. Crellin *et al.*, Regulation of cytokine secretion in human CD127(+) LTi-like innate lymphoid cells by Toll-like receptor 2. *Immunity* **33**, 752-764 (2010).
21. I. Marafini *et al.*, TNF-alpha Producing Innate Lymphoid Cells (ILCs) Are Increased in Active Celiac Disease and Contribute to Promote Intestinal Atrophy in Mice. *PLoS One* **10**, e0126291 (2015).
22. H. Xu, X. Wang, A. A. Lackner, R. S. Veazey, Type 3 innate lymphoid cell depletion is mediated by TLRs in lymphoid tissues of simian immunodeficiency virus-infected macaques. *FASEB J* **29**, 5072-5080 (2015).

23. J. Mjosberg, H. Spits, Human innate lymphoid cells. *J Allergy Clin Immunol* **138**, 1265-1276 (2016).
24. C. S. Hardman *et al.*, CD1a presentation of endogenous antigens by group 2 innate lymphoid cells. *Sci Immunol* **2**, (2017).
25. C. J. Oliphant *et al.*, MHCII-mediated dialog between group 2 innate lymphoid cells and CD4(+) T cells potentiates type 2 immunity and promotes parasitic helminth expulsion. *Immunity* **41**, 283-295 (2014).
26. T. Kobayashi *et al.*, Homeostatic Control of Sebaceous Glands by Innate Lymphoid Cells Regulates Commensal Bacteria Equilibrium. *Cell* **176**, 982-997 e916 (2019).
27. A. Negroni, M. Pierdomenico, S. Cucchiara, L. Stronati, NOD2 and inflammation: current insights. *J Inflamm Res* **11**, 49-60 (2018).
28. M. Windheim, C. Lang, M. Peggie, L. A. Plater, P. Cohen, Molecular mechanisms involved in the regulation of cytokine production by muramyl dipeptide. *Biochem J* **404**, 179-190 (2007).
29. M. Hasegawa *et al.*, A critical role of RICK/RIP2 polyubiquitination in Nod-induced NF-kappaB activation. *EMBO J* **27**, 373-383 (2008).
30. A. Sabbah *et al.*, Activation of innate immune antiviral responses by Nod2. *Nat Immunol* **10**, 1073-1080 (2009).
31. L. H. Travassos *et al.*, Nod1 and Nod2 direct autophagy by recruiting ATG16L1 to the plasma membrane at the site of bacterial entry. *Nat Immunol* **11**, 55-62 (2010).
32. Z. Al Nabhani, G. Dietrich, J. P. Hugot, F. Barreau, Nod2: The intestinal gate keeper. *PLoS Pathog* **13**, e1006177 (2017).
33. N. Nakamura *et al.*, Endosomes are specialized platforms for bacterial sensing and NOD2 signalling. *Nature* **509**, 240-244 (2014).
34. B. Thay, A. Damm, T. A. Kufer, S. N. Wai, J. Oscarsson, Aggregatibacter actinomycetemcomitans outer membrane vesicles are internalized in human host cells and trigger NOD1- and NOD2-dependent NF-kappaB activation. *Infect Immun* **82**, 4034-4046 (2014).
35. S. R. Vavricka *et al.*, hPepT1 transports muramyl dipeptide, activating NF-kappaB and stimulating IL-8 secretion in human colonic Caco2/bbe cells. *Gastroenterology* **127**, 1401-1409 (2004).
36. M. G. Netea *et al.*, Nucleotide-binding oligomerization domain-2 modulates specific TLR pathways for the induction of cytokine release. *J Immunol* **174**, 6518-6523 (2005).
37. T. P. Chapman *et al.*, Ataxin-3 Links NOD2 and TLR2 Mediated Innate Immune Sensing and Metabolism in Myeloid Cells. *Front Immunol* **10**, 1495 (2019).
38. D. Corridoni *et al.*, NOD2 and TLR2 Signal via TBK1 and PI31 to Direct Cross-Presentation and CD8 T Cell Responses. *Front Immunol* **10**, 958 (2019).
39. J. H. Fritz *et al.*, Synergistic stimulation of human monocytes and dendritic cells by Toll-like receptor 4 and NOD1- and NOD2-activating agonists. *Eur J Immunol* **35**, 2459-2470 (2005).
40. M. Baggiolini, A. Walz, S. L. Kunkel, Neutrophil-activating peptide-1/interleukin 8, a novel cytokine that activates neutrophils. *J Clin Invest* **84**, 1045-1049 (1989).
41. J. Q. Gong *et al.*, Skin colonization by Staphylococcus aureus in patients with eczema and atopic dermatitis and relevant combined topical therapy: a double-blind multicentre randomized controlled trial. *Br J Dermatol* **155**, 680-687 (2006).
42. F. Macaluso *et al.*, Polymorphisms in NACHT-LRR (NLR) genes in atopic dermatitis. *Exp Dermatol* **16**, 692-698 (2007).
43. L. Galle-Treger *et al.*, Autophagy is critical for group 2 innate lymphoid cell metabolic homeostasis and effector function. *J Allergy Clin Immunol* **145**, 502-517 e505 (2020).
44. O. Penack *et al.*, NOD2 regulates hematopoietic cell function during graft-versus-host disease. *J Exp Med* **206**, 2101-2110 (2009).

45. T. Petterson *et al.*, Effects of NOD-like receptors in human B lymphocytes and crosstalk between NOD1/NOD2 and Toll-like receptors. *J Leukoc Biol* **89**, 177-187 (2011).
46. M. Hedl, J. Li, J. H. Cho, C. Abraham, Chronic stimulation of Nod2 mediates tolerance to bacterial products. *Proc Natl Acad Sci U S A* **104**, 19440-19445 (2007).
47. C. De Salvo *et al.*, NOD2 drives early IL-33-dependent expansion of group 2 innate lymphoid cells during Crohn's disease-like ileitis. *J Clin Invest*, (2021).
48. R. Cooney *et al.*, NOD2 stimulation induces autophagy in dendritic cells influencing bacterial handling and antigen presentation. *Nat Med* **16**, 90-97 (2010).
49. S. Okumura *et al.*, Hyperexpression of NOD2 in intestinal mast cells of Crohn's disease patients: preferential expression of inflammatory cell-recruiting molecules via NOD2 in mast cells. *Clin Immunol* **130**, 175-185 (2009).
50. Y. Ogura *et al.*, Nod2, a Nod1/Apaf-1 family member that is restricted to monocytes and activates NF-kappaB. *J Biol Chem* **276**, 4812-4818 (2001).
51. A. M. Kvarnhammar, L. O. Cardell, Pattern-recognition receptors in human eosinophils. *Immunology* **136**, 11-20 (2012).
52. Y. J. Jeong *et al.*, Nod2 and Rip2 contribute to innate immune responses in mouse neutrophils. *Immunology* **143**, 269-276 (2014).
53. Y. Ogura *et al.*, Expression of NOD2 in Paneth cells: a possible link to Crohn's ileitis. *Gut* **52**, 1591-1597 (2003).
54. G. Nigro, R. Rossi, P. H. Commere, P. Jay, P. J. Sansonetti, The cytosolic bacterial peptidoglycan sensor Nod2 affords stem cell protection and links microbes to gut epithelial regeneration. *Cell Host Microbe* **15**, 792-798 (2014).
55. D. Ramanan, M. S. Tang, R. Bowcutt, P. Loke, K. Cadwell, Bacterial sensor Nod2 prevents inflammation of the small intestine by restricting the expansion of the commensal Bacteroides vulgatus. *Immunity* **41**, 311-324 (2014).
56. T. Hisamatsu *et al.*, CARD15/NOD2 functions as an antibacterial factor in human intestinal epithelial cells. *Gastroenterology* **124**, 993-1000 (2003).
57. P. Rosenstiel *et al.*, TNF-alpha and IFN-gamma regulate the expression of the NOD2 (CARD15) gene in human intestinal epithelial cells. *Gastroenterology* **124**, 1001-1009 (2003).
58. P. Hruz *et al.*, NOD2 contributes to cutaneous defense against Staphylococcus aureus through alpha-toxin-dependent innate immune activation. *Proc Natl Acad Sci U S A* **106**, 12873-12878 (2009).
59. E. Voss *et al.*, NOD2/CARD15 mediates induction of the antimicrobial peptide human beta-defensin-2. *J Biol Chem* **281**, 2005-2011 (2006).
60. N. Warner *et al.*, A genome-wide siRNA screen reveals positive and negative regulators of the NOD2 and NF-kappaB signaling pathways. *Sci Signal* **6**, rs3 (2013).
61. A. Lecat *et al.*, The c-Jun N-terminal kinase (JNK)-binding protein (JNKBP1) acts as a negative regulator of NOD2 protein signaling by inhibiting its oligomerization process. *J Biol Chem* **287**, 29213-29226 (2012).
62. K. H. Lee, A. Biswas, Y. J. Liu, K. S. Kobayashi, Proteasomal degradation of Nod2 protein mediates tolerance to bacterial cell wall components. *J Biol Chem* **287**, 39800-39811 (2012).
63. S. Lipinski *et al.*, RNAi screening identifies mediators of NOD2 signaling: implications for spatial specificity of MDP recognition. *Proc Natl Acad Sci U S A* **109**, 21426-21431 (2012).
64. A. L. Richmond *et al.*, The nucleotide synthesis enzyme CAD inhibits NOD2 antibacterial function in human intestinal epithelial cells. *Gastroenterology* **142**, 1483-1492 e1486 (2012).
65. L. Campbell, H. Williams, R. A. Crompton, S. M. Cruickshank, M. J. Hardman, Nod2 deficiency impairs inflammatory and epithelial aspects of the cutaneous wound-healing response. *J Pathol* **229**, 121-131 (2013).

66. M. Fazli *et al.*, Nonrandom distribution of Pseudomonas aeruginosa and Staphylococcus aureus in chronic wounds. *J Clin Microbiol* **47**, 4084-4089 (2009).
67. H. Williams *et al.*, Cutaneous Nod2 Expression Regulates the Skin Microbiome and Wound Healing in a Murine Model. *J Invest Dermatol* **137**, 2427-2436 (2017).
68. X. Wu *et al.*, Comparative genomics and functional analysis of niche-specific adaptation in Pseudomonas putida. *FEMS Microbiol Rev* **35**, 299-323 (2011).
69. C. L. Feerick, D. P. McKernan, Understanding the regulation of pattern recognition receptors in inflammatory diseases - a 'Nod' in the right direction. *Immunology* **150**, 237-247 (2017).
70. C. R. Homer, A. L. Richmond, N. A. Rebert, J. P. Achkar, C. McDonald, ATG16L1 and NOD2 interact in an autophagy-dependent antibacterial pathway implicated in Crohn's disease pathogenesis. *Gastroenterology* **139**, 1630-1641, 1641 e1631-1632 (2010).
71. G. Muzes, Z. Tulassay, F. Sipos, Interplay of autophagy and innate immunity in Crohn's disease: a key immunobiologic feature. *World J Gastroenterol* **19**, 4447-4454 (2013).
72. A. Negroni *et al.*, NOD2 induces autophagy to control AIEC bacteria infectiveness in intestinal epithelial cells. *Inflamm Res* **65**, 803-813 (2016).
73. K. Cadwell, Crohn's disease susceptibility gene interactions, a NOD to the newcomer ATG16L1. *Gastroenterology* **139**, 1448-1450 (2010).
74. H. T. Nguyen, P. Lapaquette, M. A. Bringer, A. Darfeuille-Michaud, Autophagy and Crohn's disease. *J Innate Immun* **5**, 434-443 (2013).
75. M. Salem, M. Ammitzboell, K. Nys, J. B. Seidelin, O. H. Nielsen, ATG16L1: A multifunctional susceptibility factor in Crohn disease. *Autophagy* **11**, 585-594 (2015).
76. P. K. Anand *et al.*, TLR2 and RIP2 pathways mediate autophagy of Listeria monocytogenes via extracellular signal-regulated kinase (ERK) activation. *J Biol Chem* **286**, 42981-42991 (2011).
77. R. J. Chen, Y. H. Lee, Y. L. Yeh, Y. J. Wang, B. J. Wang, The Roles of Autophagy and the Inflammasome during Environmental Stress-Triggered Skin Inflammation. *Int J Mol Sci* **17**, (2016).
78. J. P. Hugot *et al.*, Association of NOD2 leucine-rich repeat variants with susceptibility to Crohn's disease. *Nature* **411**, 599-603 (2001).
79. C. Miceli-Richard *et al.*, CARD15 mutations in Blau syndrome. *Nat Genet* **29**, 19-20 (2001).
80. N. Kanazawa *et al.*, Early-onset sarcoidosis and CARD15 mutations with constitutive nuclear factor-kappaB activation: common genetic etiology with Blau syndrome. *Blood* **105**, 1195-1197 (2005).
81. D. J. Philpott, M. T. Sorbara, S. J. Robertson, K. Croitoru, S. E. Girardin, NOD proteins: regulators of inflammation in health and disease. *Nat Rev Immunol* **14**, 9-23 (2014).
82. W. Strober, N. Asano, I. Fuss, A. Kitani, T. Watanabe, Cellular and molecular mechanisms underlying NOD2 risk-associated polymorphisms in Crohn's disease. *Immunol Rev* **260**, 249-260 (2014).
83. Y. Ogura *et al.*, A frameshift mutation in NOD2 associated with susceptibility to Crohn's disease. *Nature* **411**, 603-606 (2001).
84. W. Jiang *et al.*, Recognition of gut microbiota by NOD2 is essential for the homeostasis of intestinal intraepithelial lymphocytes. *J Exp Med* **210**, 2465-2476 (2013).
85. A. Couturier-Maillard *et al.*, NOD2-mediated dysbiosis predisposes mice to transmissible colitis and colorectal cancer. *J Clin Invest* **123**, 700-711 (2013).
86. T. Sidiq, S. Yoshihama, I. Downs, K. S. Kobayashi, Nod2: A Critical Regulator of Ileal Microbiota and Crohn's Disease. *Front Immunol* **7**, 367 (2016).
87. D. Jiao *et al.*, NOD2 and TLR2 ligands trigger the activation of basophils and eosinophils by interacting with dermal fibroblasts in atopic dermatitis-like skin inflammation. *Cell Mol Immunol* **13**, 535-550 (2016).

88. C. K. Wong, I. M. Chu, K. L. Hon, M. S. Tsang, C. W. Lam, Aberrant Expression of Bacterial Pattern Recognition Receptor NOD2 of Basophils and Microbicidal Peptides in Atopic Dermatitis. *Molecules* **21**, 471 (2016).
89. S. A. Roth, M. Simanski, F. Rademacher, L. Schroder, J. Harder, The pattern recognition receptor NOD2 mediates Staphylococcus aureus-induced IL-17C expression in keratinocytes. *J Invest Dermatol* **134**, 374-380 (2014).
90. A. A. Navarini, L. E. French, G. F. Hofbauer, Interrupting IL-6-receptor signaling improves atopic dermatitis but associates with bacterial superinfection. *J Allergy Clin Immunol* **128**, 1128-1130 (2011).
91. A. Toshitani, J. C. Ansel, S. C. Chan, S. H. Li, J. M. Hanifin, Increased interleukin 6 production by T cells derived from patients with atopic dermatitis. *J Invest Dermatol* **100**, 299-304 (1993).

Acknowledgements: We thank the staff of the WIMM flow cytometry facility, especially Craig Waugh. We are grateful to all suction blister, blood, and skin donors and to Churchill hospital Dermatology Department research nurses, especially Melanie Westmoreland and Teena Mackenzie. We thank all the patients who contributed to this study and the generous support of A. Simmons' clinical research nurses led by S. Fourie.

Funding: We acknowledge the support of the National Institute for Health Research Clinical Research Network, British Association of Dermatologists, British Skin Foundation, and Misses Barrie Charitable Trust. This work was funded by the Medical Research Council (CF7720, U105178805, MR/K018779/1) and the Wellcome Trust (090532/Z/09/Z), and supported by the NIHR (NIHR) Oxford Biomedical Research Centre (BRC). D. Cousins acknowledges support from the NIHR Leicester Biomedical Research Centre. A. Simmons was supported by an NIHR Senior Investigator Award and Wellcome Investigator Award, D. Corridoni was supported by Crohn's and Colitis UK. The views expressed are those of the authors and not necessarily those of the NHS, the NIHR or the Department of Health.

Author contributions: C.S.H. Y.C. M.S. J.N. D.C. M.J. C.F. J.L.B. D.J.C. and G.O. performed experiments. E.R. carried out bioinformatic analysis of RNA Sequencing data. A.S. and D.J. provided invaluable samples. A.N.M. D.J.C. A.S. D.C. and J.L.B. provided feedback and supervised aspects of the study. C.S.H. and G.O. conceived the study and wrote the manuscript. C.S.H completed the statistical analysis of data.

Competing interests: G. Ogg has served on advisory boards or holds consultancies or equity with Eli Lilly, Novartis, Janssen, Orbit Discovery and UCB Pharma, and has undertaken clinical trials

for Atopix, Regeneron/Sanofi, Roche, Anaptysbio. A. McKenzie has received grant support from Medimmune/AstraZeneca and GSK. The authors declare no further competing financial interests.

Figures

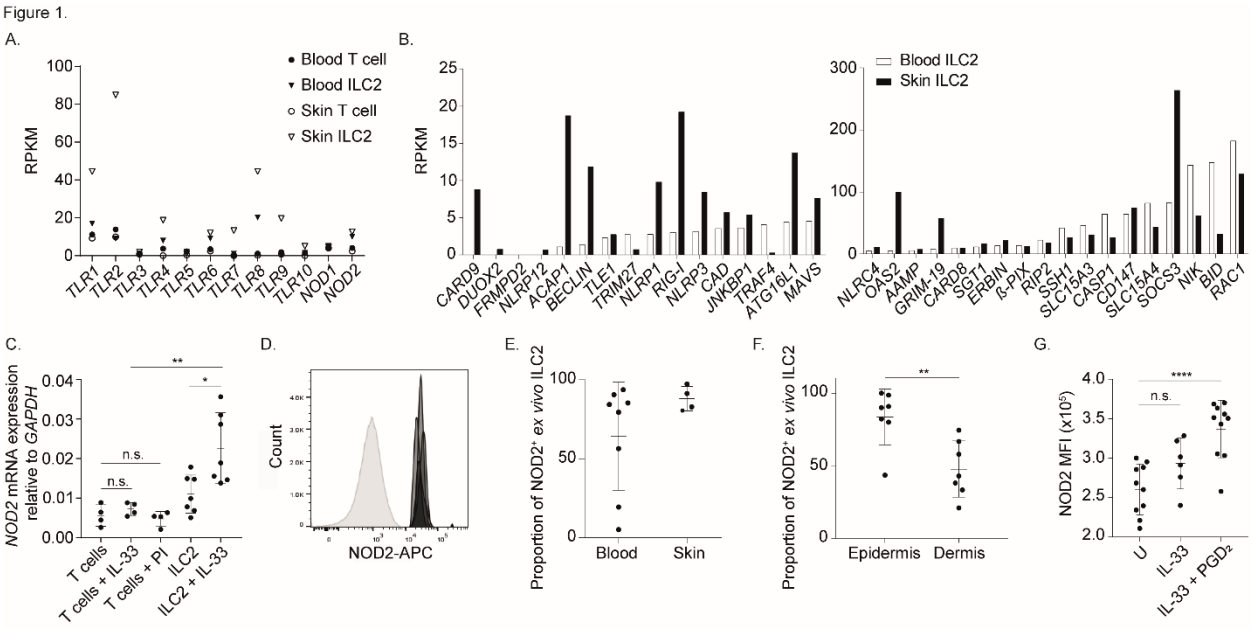

Figure 1. Human ILC2 express pattern recognition receptor NOD2. **A.** PRR gene expression of skin blister and blood-derived ILC2 and T cells determined by RNA-Seq and measured in Reads Per Kilobase of transcript per Million mapped reads (RPKM) following 24 hour *in vivo* HDM blister challenge on the arm of a HDM-sensitive healthy index participant (n=1). **B.** NOD2 binding partner gene expression of skin blister and blood-derived ILC2 determined by RNA-Seq and measured in RPKM following 24 hour *in vivo* HDM blister challenge (n=1). **C.** RT-PCR analysis of *NOD2* gene expression by ILC2 or T cells following stimulation with IL-33 (50ng/ml) and/or PGD_2 (100nM), or PMA (15 ng / ml) and ionomycin (7.5 ng / ml) (PI) (n=4-7, one-way ANOVA with Tukey's, data representative of 3 independent experiments). Gene expression normalized to *GAPDH*. **D.** NOD2 protein expression in human blood ILC2 measured by flow cytometry. Pale grey fill represents FMO isotype control. Darker grey fill, representative blood-derived ILC2 donor NOD2 expression (n=4). **E.** Summary of ILC2 NOD2 expression by human PBMC and

skin biopsy samples, analyzed by flow cytometry (n=4-8, data representative of at least 4 independent experiments). **F.** Summary of NOD2 expression by ILC2 derived from human skin localized within the epidermis and dermis, analyzed by flow cytometry (n=7, data representative of 4 independent experiments). **G.** Flow cytometry analysis of NOD2 protein expression intensity by ILC2 following stimulation with IL-33 (50ng/ml) and/or PGD_2 (100nM) as measured by MFI (n=4, t-test, data representative of 3 independent experiments).

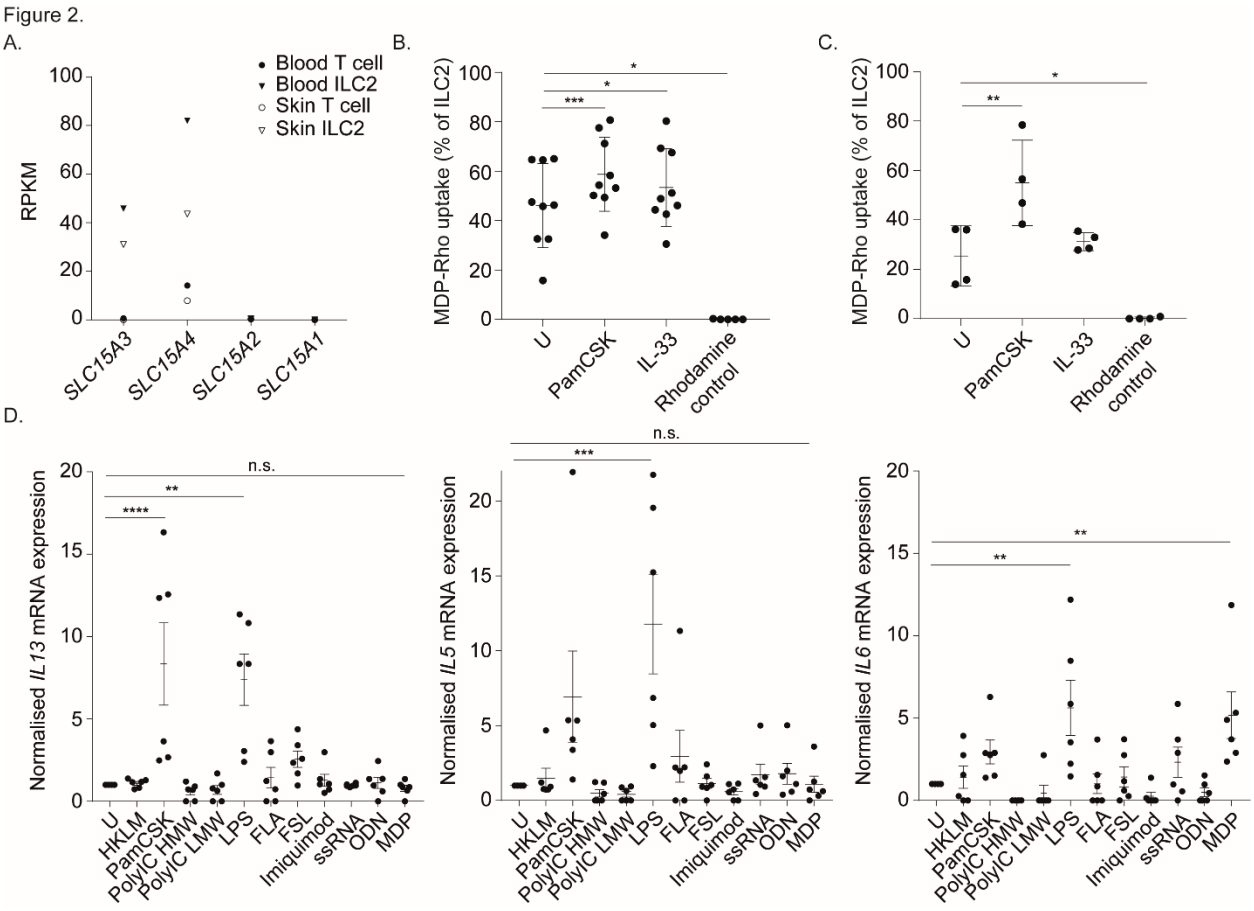

Figure 2. ILC2 are capable of functional NOD2 signaling. A. MDP transporter gene expression of skin blister and blood derived ILC2 and T cells determined by RNA-Seq and measured in Reads Per Kilobase of transcript per Million mapped reads (RPKM) following 24 hour *in vivo* HDM blister challenge of a HDM-sensitive healthy index participant (n=1). **B.** MDP-rhodamine (MDP-Rho, 5µg/ml, or Rhodamine B control) uptake measured following 3 hour coculture with ILC2, with/without prior stimulation (1 hour) with Pam_3CSK_4 (10µg/ml) or IL-33 (50ng/ml) measured by flow cytometry (n=9, paired one-way ANOVA with Dunnett's, data representative of 3 independent experiments) or **C.** confocal microscopy (data quantified for n=2 donors, 2 images (5x5 tiles) per donor, one-way ANOVA with Dunnett's). **D.** RT- PCR analysis of cytokine gene expression by ILC2 following 6 hour stimulation with panel of PRR agonists. Gene expression

normalized to *GAPDH* (n=6, one-way ANOVA with Dunnett's multiple comparison test, data representative of at least 4 independent experiments).

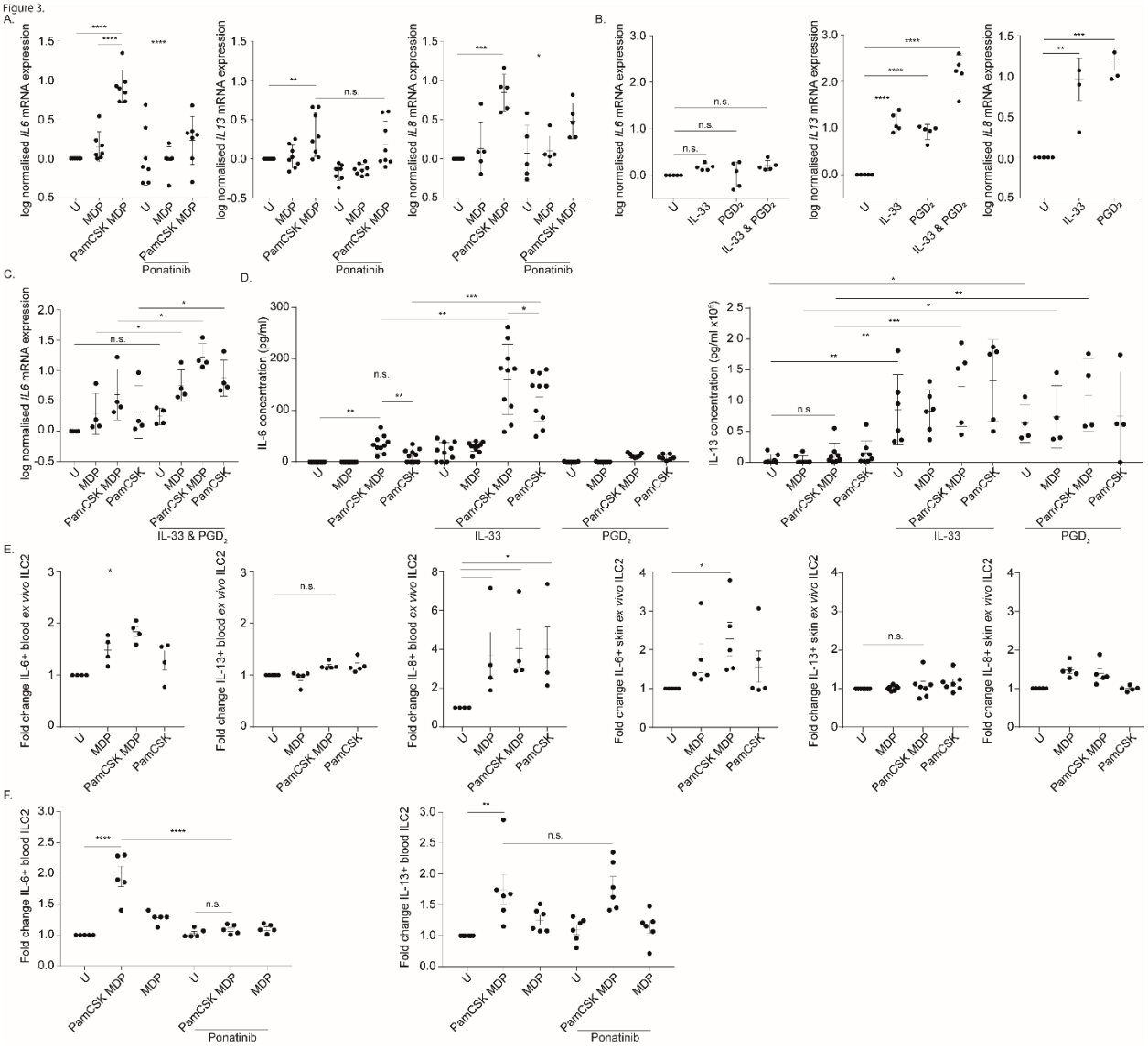

Figure 3. ILC2 NOD2 signaling induces an IL-6 effector cytokine bias. A. The effect of NOD2 signaling inhibition by ponatinib (25nM, 1 hour) on 6 hour stimulation with MDP (1µg/ml) and/or Pam_3CSK_4 (10µg/ml) on ILC2 cytokine gene expression, measured by real-time PCR analysis. Gene expression normalized to *GAPDH*. (n=8, one-way ANOVA with Dunnett's of Tukey's multiple comparison test, data representative of at least 4 independent experiments). **B.** Real-time PCR analysis of cytokine gene expression by ILC2 following 6 hour stimulation with IL-33

(50ng/ml) and PGD_2 (100nM). Gene expression normalized to *GAPDH*. (n=3-7, one-way ANOVA with Dunnett's multiple comparison test, data representative of at least 4 independent experiments). **C-D.** Induction of ILC2 cytokine expression measured by (C.) real-time PCR following 6 hour stimulation or D. ELISA following 5 day stimulation with MDP (1µg/ml), Pam_3CSK_4 (10µg/ml), and/or IL-33 (50ng/ml) and PGD_2 (100nM). (n=4 or 10 respectively, one-way ANOVA with Tukey's multiple comparison test, data representative of at least 4 independent experiments). **E.** ILC2 cytokine protein production assessed *ex vivo* by intracellular flow cytometry after 24 hour stimulation of PBMC (left) and skin biopsy-derived mononuclear cells (right) with MDP (1µg/ml), Pam_3CSK_4 (10µg/ml), IL-33 (50ng/ml) or PGD_2 (100nM). (n=5-7, one-way ANOVA with Dunnett's multiple comparison test, data representative of at least 4 independent experiments). **F.** The effect of NOD2 signaling inhibition by ponatinib (25nM, 1 hour) on 24 hour stimulation with MDP (1µg/ml) and/or Pam_3CSK_4 (10µg/ml) on ILC2 cytokine gene expression measured by intracellular flow cytometry. Expressed as fold changed. (n=5-6, one-way ANOVA with Sidak's multiple comparison test, data representative of at least 4 independent experiments).

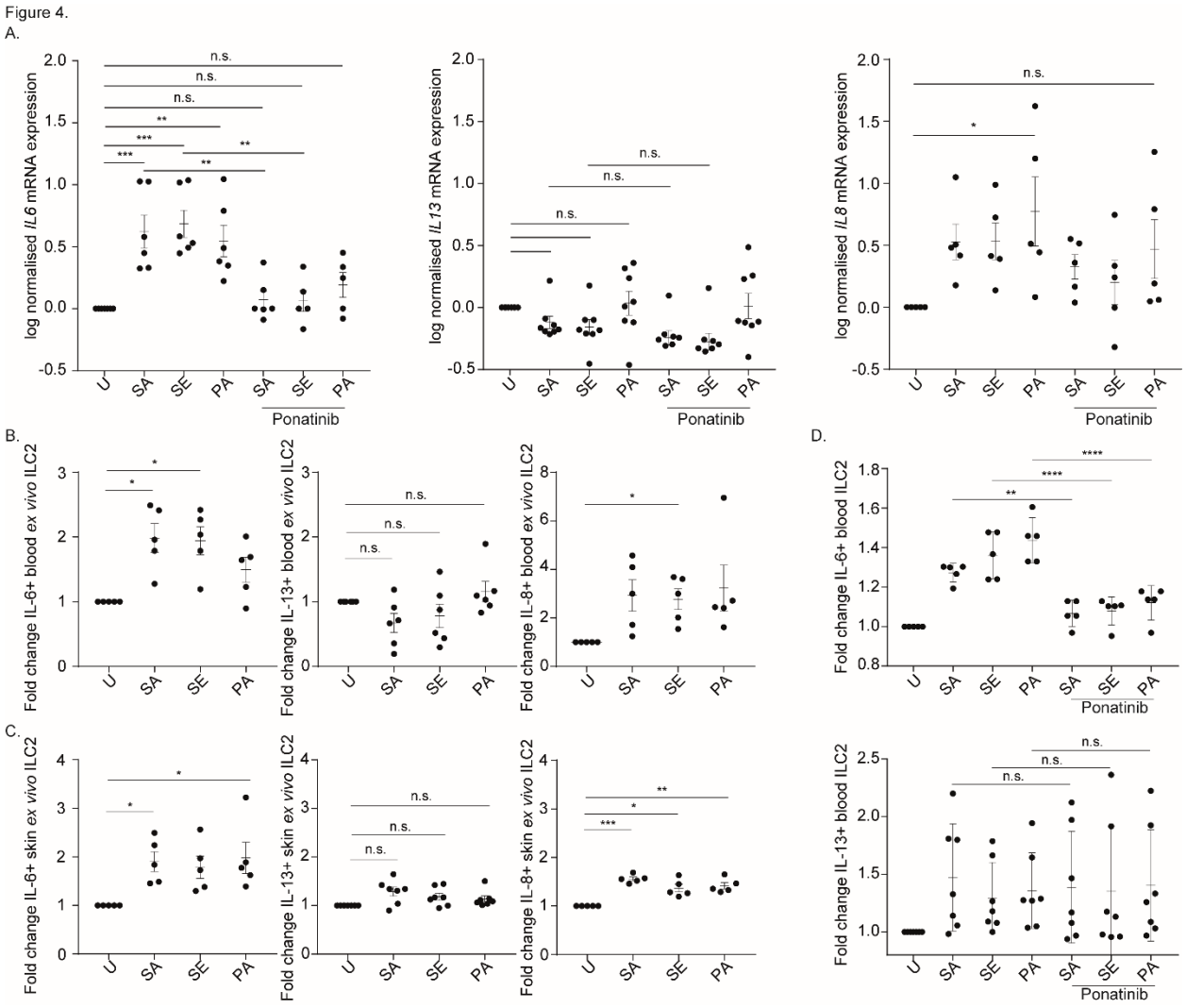

Figure 4. ILC2 sense bacterial components directly via NOD2. A. The effect of NOD2 signaling inhibition by ponatinib (25nM, 1 hour) on 6 hour stimulation with heat-killed preparations of SA (*S. aureus* 10^8cells/ml), SE (*S. epidermidis* 10^8cells/ml) or PA (*P. aeruginosa* 10^8cells/ml) on ILC2 cytokine gene expression measured by real-time PCR analysis. Gene expression normalized to *GAPDH*. (n=5-7, one-way ANOVA with Tukey's multiple comparison test, data representative of at least 4 independent experiments). **B-C.** Summary of ILC2 cytokine protein production assessed *ex vivo* by intracellular flow cytometry after 24 hour stimulation of PBMC (**B.**) and skin biopsy-derived mononuclear cells (**C**.) with heat-killed preparations of SA (*S. aureus*), SE (*S. epidermidis*) or PA (*P. aeruginosa*) (n=5-7, one-way ANOVA with Dunnett's

multiple comparison test, data representative of at least 4 independent experiments). **D.** The effect of NOD2 signaling inhibition by ponatinib (25nM) 1 hour prior to 24 hour stimulation with heat-killed preparations of SA (*S. aureus*), SE (*S. epidermidis*) or PA (*P. aeruginosa*) on ILC2 cytokine gene expression measured by intracellular flow cytometry. Expressed as fold change, (n=5-6, one-way ANOVA with Sidak's multiple comparison test, data representative of at least 4 independent experiments).

Figure 5.

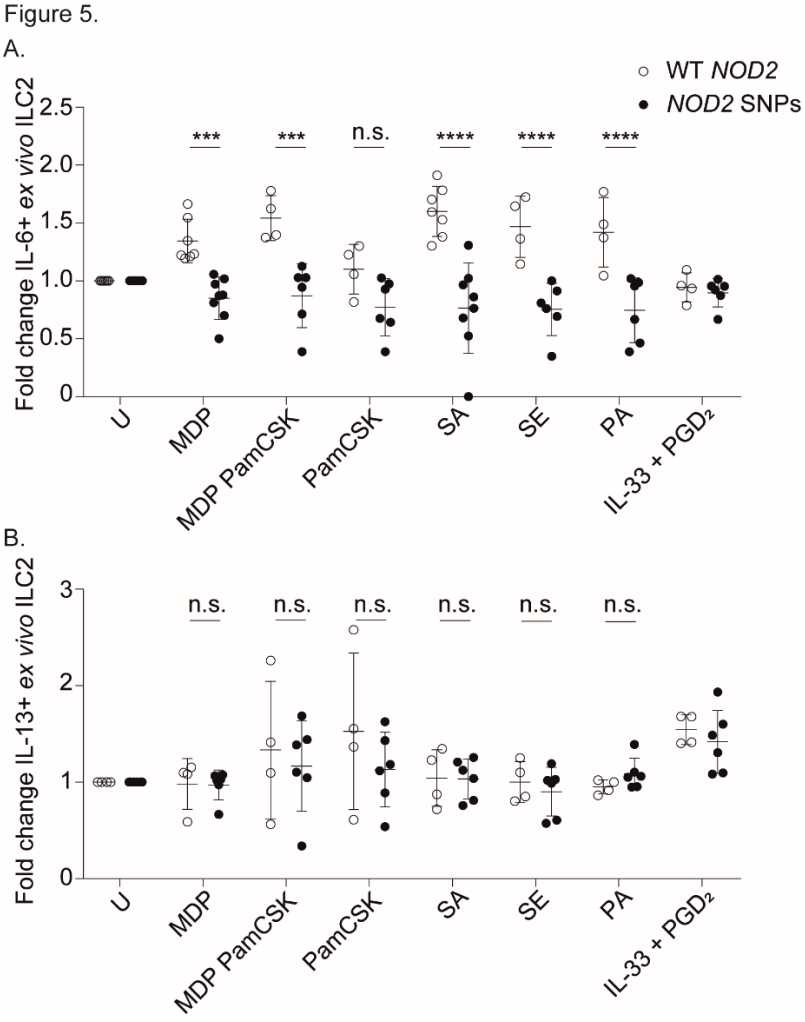

Figure 5. *NOD2* mutation reduces ILC2 capacity to produce IL-6. Induction of ILC2-derived IL-6 **(A.)** and IL-13 **(B.)** following 24 hour stimulation with MDP (1µg/ml), Pam_3CSK_4 (10µg/ml), IL-33 (50ng/ml) or PGD_2 (100nM), heat-killed preparations of SA (*S. aureus*), SE (*S. epidermidis*) or PA (*P. aeruginosa*) measured by intracellular flow cytometry in PBMC from healthy volunteers with wild-type *NOD2* gene expression (WT *NOD2*) or patients with loss of function *NOD2* mutations (*NOD2* SNPs). (n=4-8, one-way ANOVA with Sidak's multiple comparison test, data representative of at least 6 independent experiments).

Figure 6.

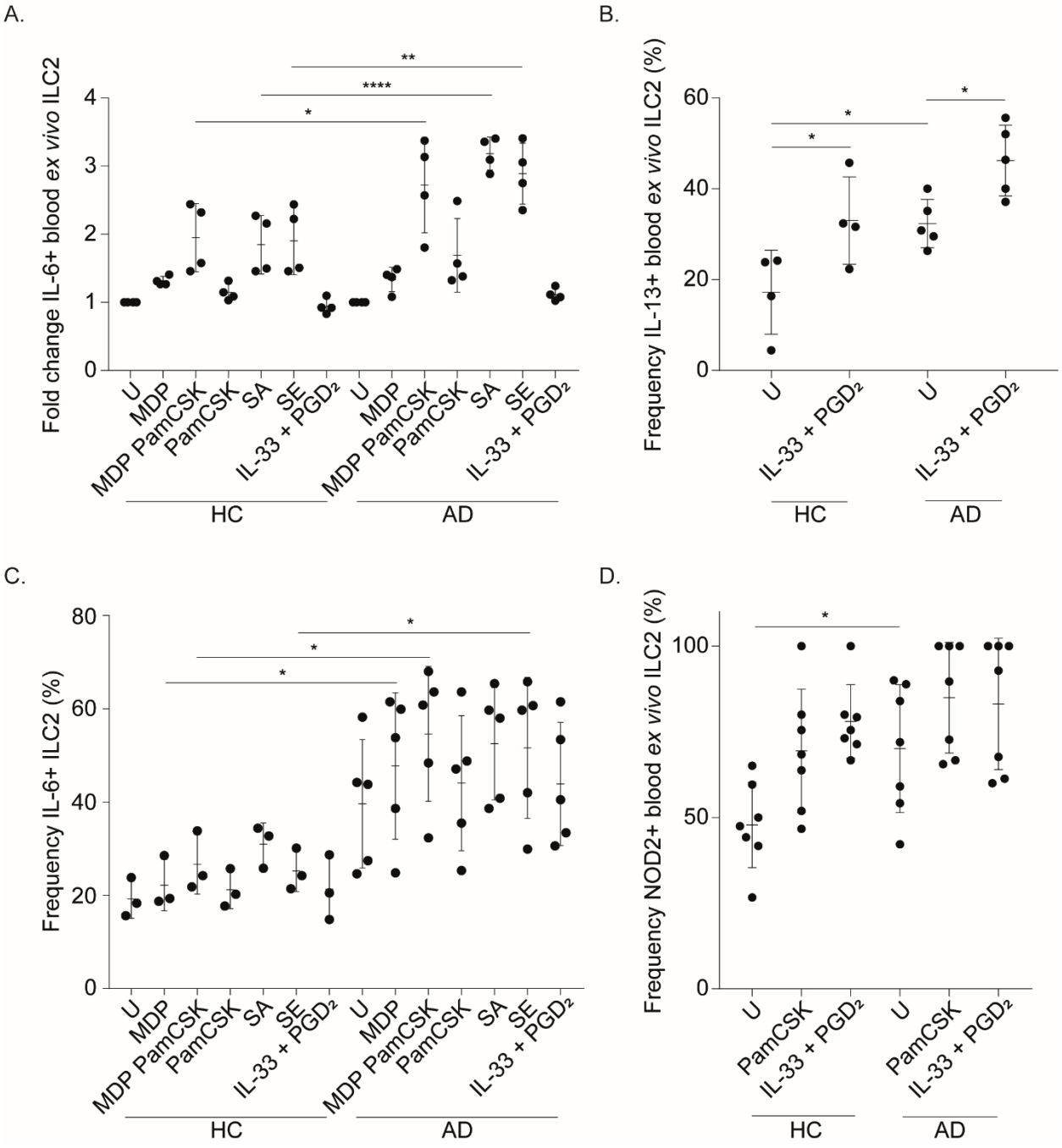

Figure 6. Atopic dermatitis patient derived ILC2 exhibit enhanced NOD2 dependent IL-6 production. A. Induction of ILC2-derived IL-6 **(A.)** and IL-13 **(B.)** following 24 hour stimulation with MDP (1µg/ml), Pam_3CSK_4 (10µg/ml), heat-killed preparations of SA (*S. aureus*), SE (*S.*

epidermidis) or IL-33 (50ng/ml) and PGD_2 (100nM), measured by intracellular flow cytometry in PBMC from healthy volunteers (HC) or patients with atopic dermatitis (AD). (n=4, one-way ANOVA with Sidak's multiple comparison test, data representative of 3 independent experiments. **C.** Induction of ILC2-derived IL-6 following 24 hour stimulation with MDP (1µg/ml), Pam_3CSK_4 (10µg/ml), heat-killed preparations of SA (*S. aureus*), SE (*S. epidermidis*) or IL-33 (50ng/ml) and PGD_2 (100nM), measured by intracellular flow cytometry in ILC2 isolated and expanded from healthy volunteers (HC) or patients with atopic dermatitis (AD). (n=3-5, one-way ANOVA with Sidak's multiple comparison test, data representative of 3 independent experiments). **D.** NOD2 protein expression following 24 hour stimulation with Pam_3CSK_4 (10µg/ml) or IL-33 (50ng/ml) and PGD_2 (100nM), measured by intracellular flow cytometry in PBMC from healthy volunteers (HC) or patients with atopic dermatitis (AD). (n=7, one-way ANOVA with Tukey's multiple comparison test, data representative of 3 independent experiments.

Figure 7.

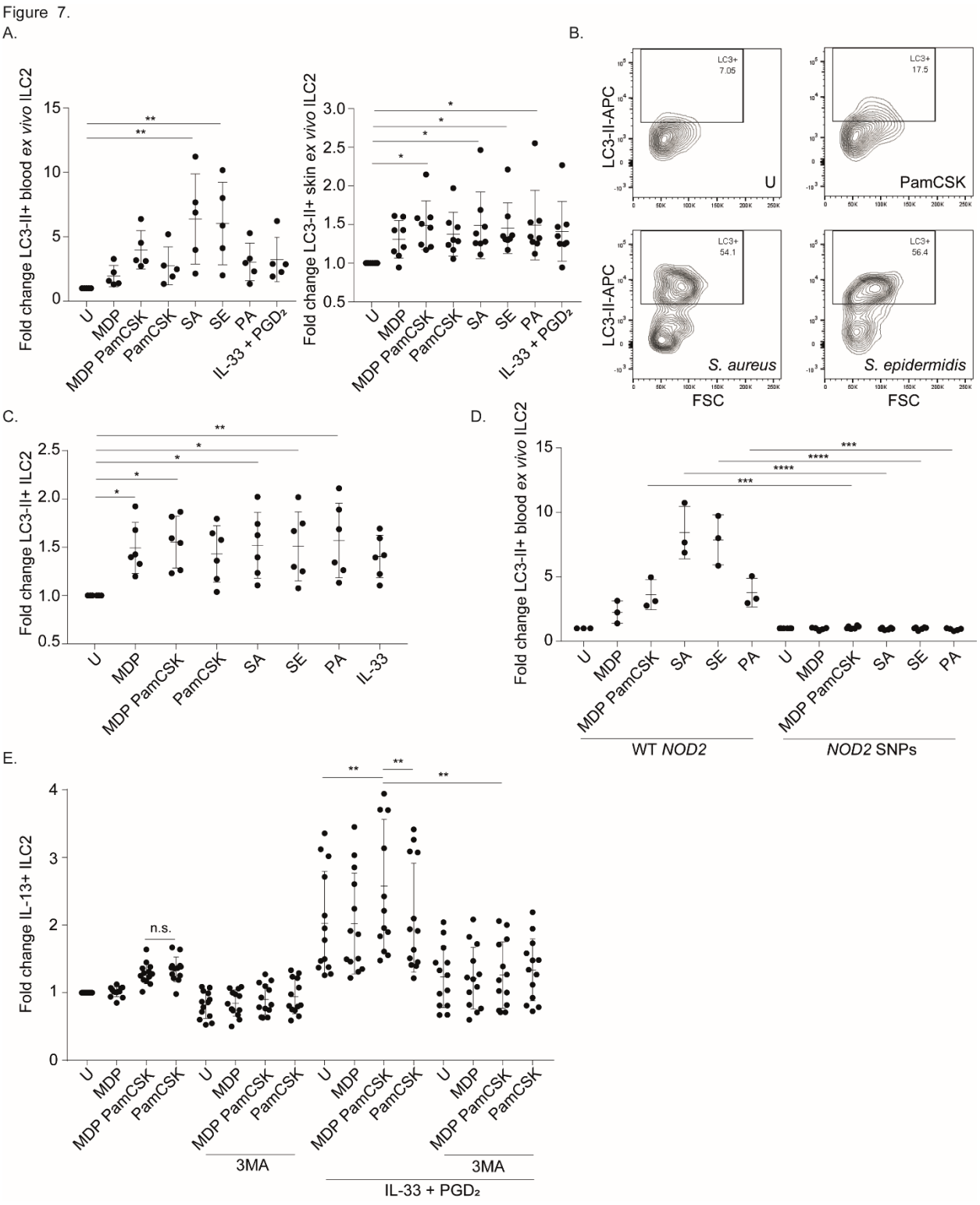

Figure 7. Bacterial stimulation of ILC2 induces autophagy via NOD2. A. Summary of ILC2 autophagy assessed *ex vivo* by intracellular flow cytometry staining of LC3-II after 24 hour

stimulation of PBMC and skin-biopsy derived mononuclear cells with heat-killed preparations of SA (*S. aureus*), SE (*S. epidermidis*) or PA (*P. aeruginosa*) and **B.** Representative flow cytometry plots of skin biopsy-derived ILC2. (n=5-9, one-way ANOVA with Dunnett's multiple comparison test, data representative of at least 5 independent experiments). **C.** Summary of ILC2 autophagy assessed in purified human blood ILC2 by intracellular flow cytometry staining of LC3-II after 24 hour stimulation with MDP (1µg/ml), Pam_3CSK_4 (10µg/ml), IL-33 (50ng/ml) or PGD_2 (100nM), heat-killed preparations of SA (*S. aureus*), SE (*S. epidermidis*) or PA (*P. aeruginosa*). (n=6, one-way ANOVA with Dunnett's multiple comparison test, data representative of 3 independent experiments). **D.** Induction of ILC2-LC3-II following 24 hour stimulation with MDP (1µg/ml), Pam_3CSK_4 (10µg/ml), heat-killed preparations of SA (*S. aureus*), SE (*S. epidermidis*) or PA (*P. aeruginosa*) measured by intracellular flow cytometry in PBMC from healthy volunteers with wild-type *NOD2* gene expression (WT *NOD2*) or patients with loss of function *NOD2* mutations (*NOD2* SNPs). (n=3-6, one-way ANOVA with Sidak's multiple comparison test, data representative of 3 independent experiments). **E.** The effect of autophagy inhibition by 3-Methyladenine (5mM, 1 hour) on 6 hour stimulation with MDP (1µg/ml), Pam_3CSK_4 (10µg/ml), IL-33 (50ng/ml) or PGD_2 (100nM) on ILC2 IL-13 induction measured by flow cytometry. (n=8 donors, one-way ANOVA with Tukey's multiple comparison test, data representative of 4 independent experiments).

Supplementary Materials

Figure S1.

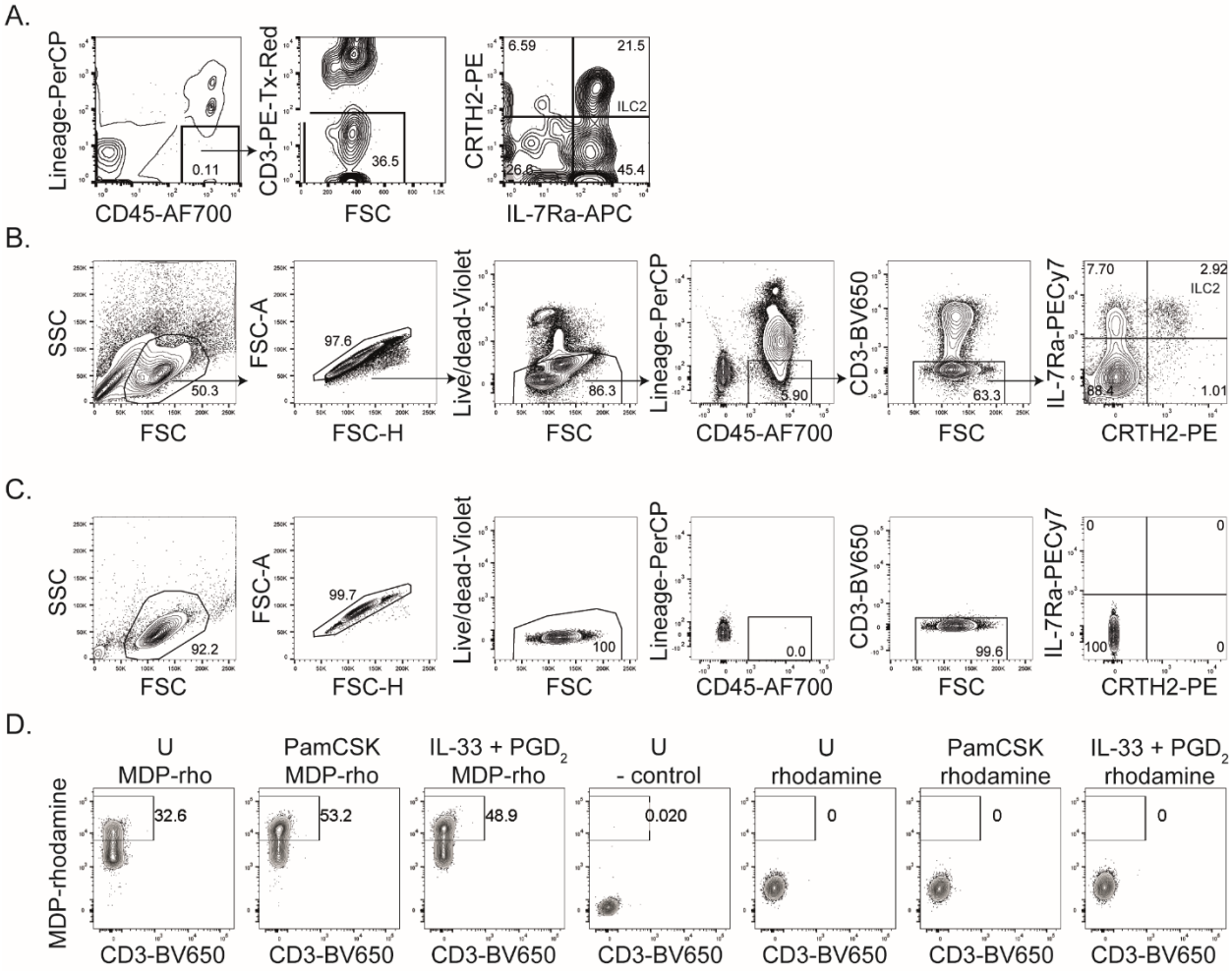

Figure S1. Isolation of Skin Blister ILC2. **A.** Flow cytometry antibody stain for skin blister ILC2. ILC2 are $CD45^+/CD3^-/Lineage^-/CRTH2^+/IL\text{-}7R\alpha^+$. **B.** Full gating strategy for isolation and analysis of blood ILC2. **C.** Isotype controls for strategy of isolation and analysis of ILC2. **D.** Representative flow cytometry plots for ILC2 uptake of MDP-Rhodamine. ILC2 were pre-stimulated as indicated with Pam_3CSK_4 (10µg/ml) or IL-33 and PGD_2 (50ng/ml and 100nM) (U: unstimulated) for 1 hour prior to addition of MDP-rhodamine (MDP-Rho, 5µg/ml for 3 hours), unconjugated rhodamine (rhodamine, 5µg/ml for 3 hours) or media alone (- control).

Figure S2.

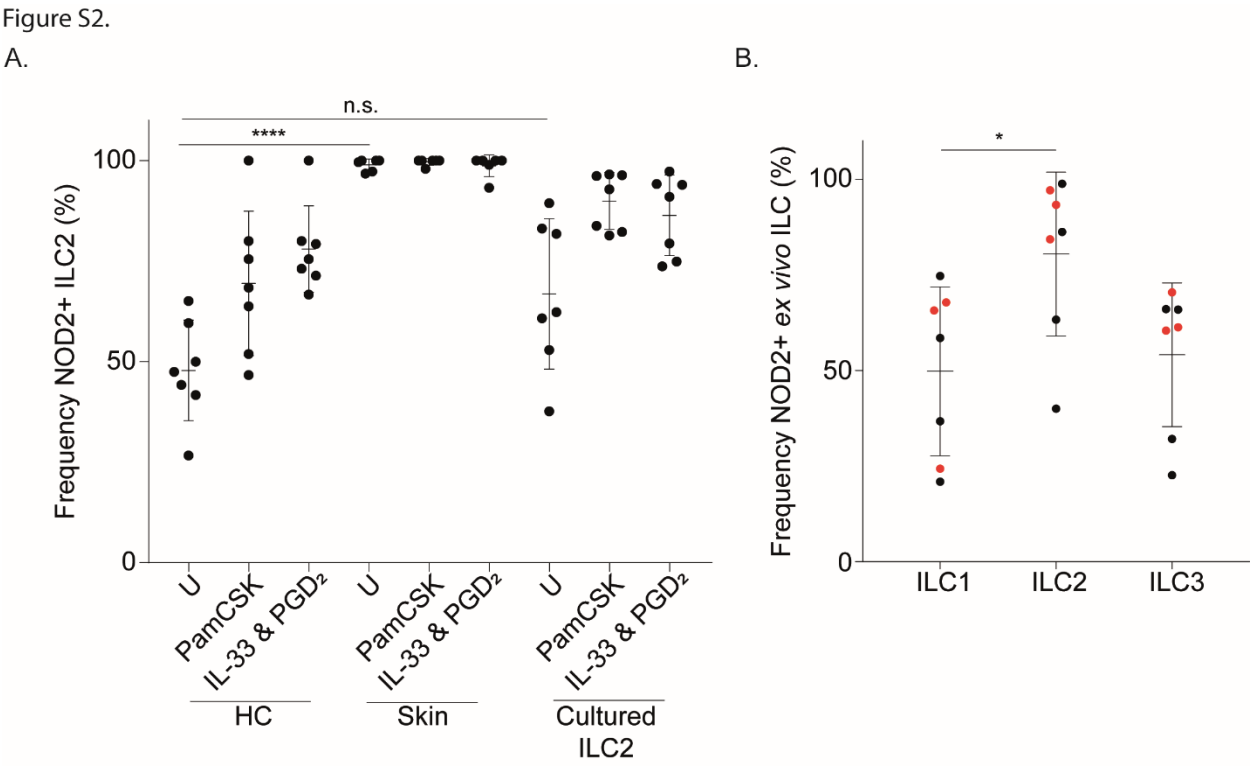

Figure S2. NOD2 expression analysis of ILC2. A. Flow cytometry analysis of NOD2 protein in ILC2 from different sources, (HC: *ex vivo* blood analysis, Skin: *ex vivo* skin analysis and Cultured ILC2: ILC2 which have been isolated, expanded and cultured for 6-8 weeks). ILC2 were stimulated for 24 hours with Pam_3CSK_4 (10µg/ml) or IL-33 (50ng/ml) and PGD_2 (100nM) (n=7, one-way ANOVA with Tukey's multiple comparison test, data representative of 5 independent experiments). **B.** Flow cytometry analysis of NOD2 protein in ILC subsets *ex vivo* within PBMC and skin biopsy-derived mononuclear cells. (n=4 blood donors (black) and n=3 skin donors (red), one-way ANOVA with Tukey's multiple comparison test, data representative of 3 independent experiments).

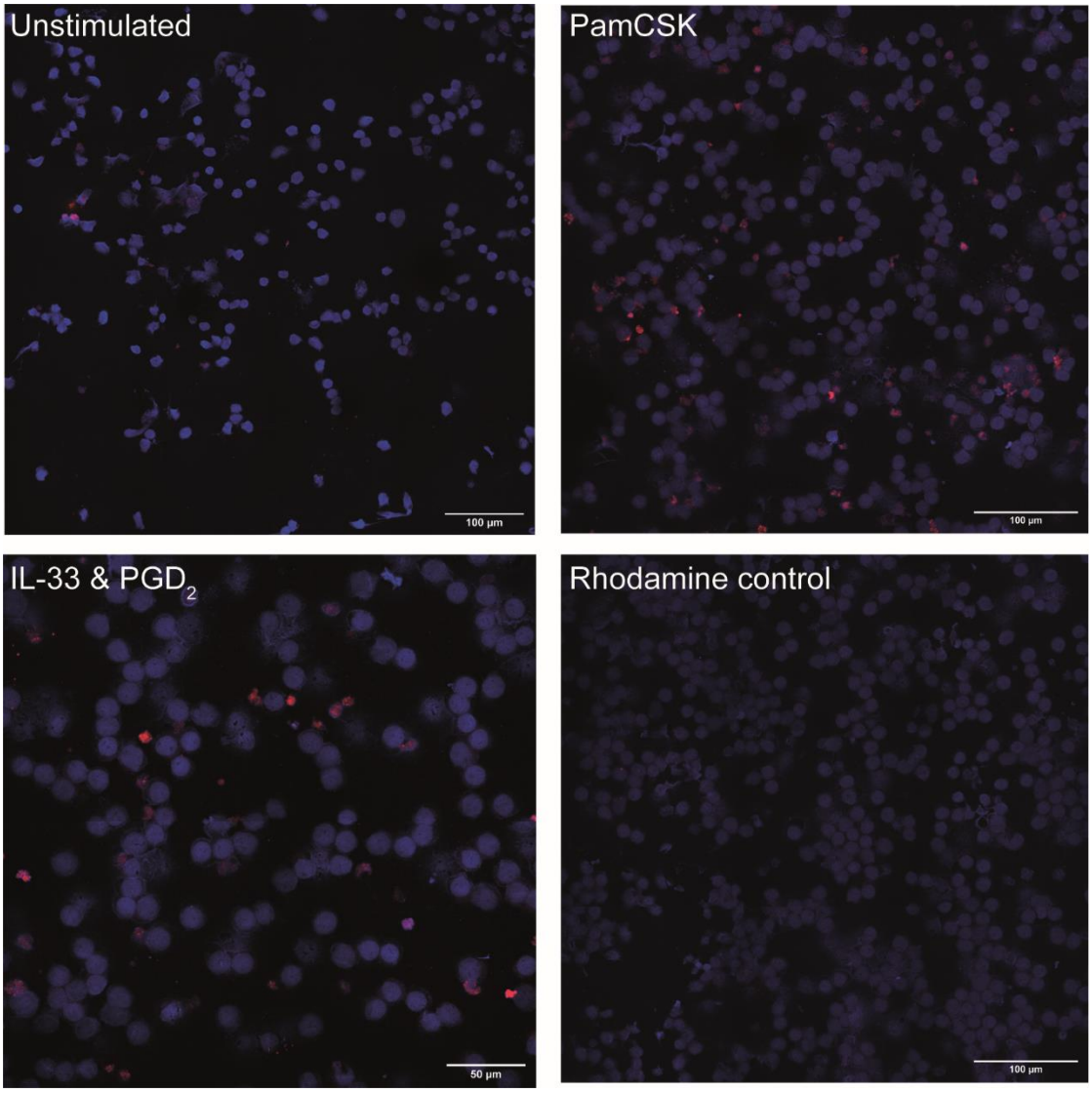

Figure S3. Imaging of MDP-rhodamine uptake by activated ILC2. Representative confocal microscopy images of blood-derived ILC2 cytospins. ILC2 were pre-stimulated for 1 hour as indicated with Pam_3CSK_4 (10µg/ml) or IL-33 (50ng/ml) and PGD_2 (100nM) and then incubated for 3 hours with MDP-rhodamine (5µg/ml, or unconjugated rhodamine control).

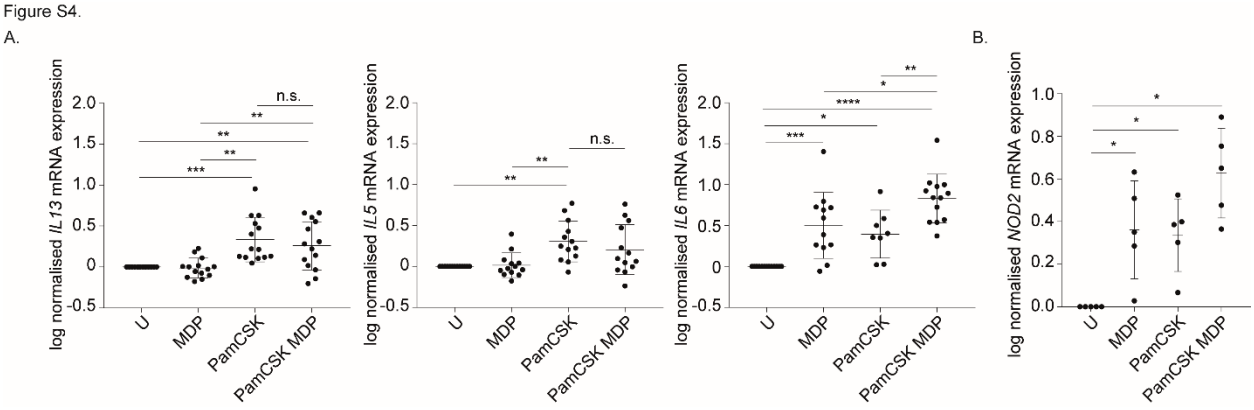

Figure S4. NOD2 and TLR2 stimulation of ILC2. Real-time PCR analysis of **A.** cytokine or **B.** NOD2 gene expression by ILC2 following 6 hour stimulation with MDP (1µg/ml) and/or Pam_3CSK_4 (10µg/ml). Gene expression normalized to *GAPDH*. (n=5-13, one-way ANOVA with Tukey's multiple comparison test, data representative of 5 independent experiments).

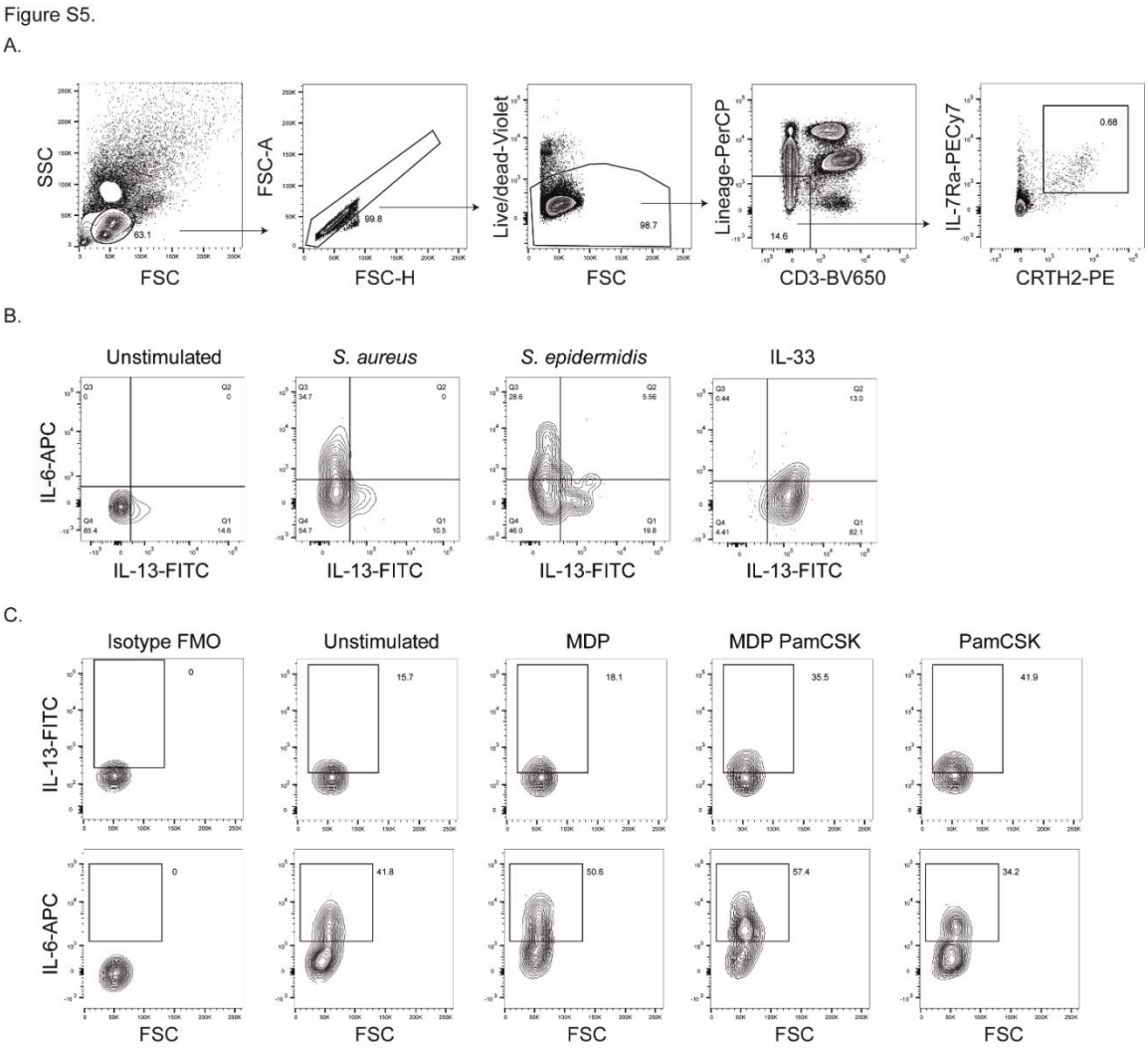

Figure S5. Skin resident bacterial preparation stimulation of ILC2. A. Full gating strategy for analysis of skin biopsy ILC2. **B.** Representative flow cytometry plots of ILC2 cytokine protein production assessed *ex vivo* by intracellular flow cytometry after 24 hour stimulation of skin biopsy-derived mononuclear cells with heat-killed preparations of *S. aureus* or *S. epidermidis*, or IL-33 (50ng/ml). **C.** Isotype FMO control and representative flow cytometry plots of gating strategy for detection of ILC2 cytokine production following 24 hour stimulation with MDP (1µg/ml) and/or Pam_3CSK_4 (10µg/ml) measured by intracellular flow cytometry in PBMCs from a healthy volunteer.

Figure S6.

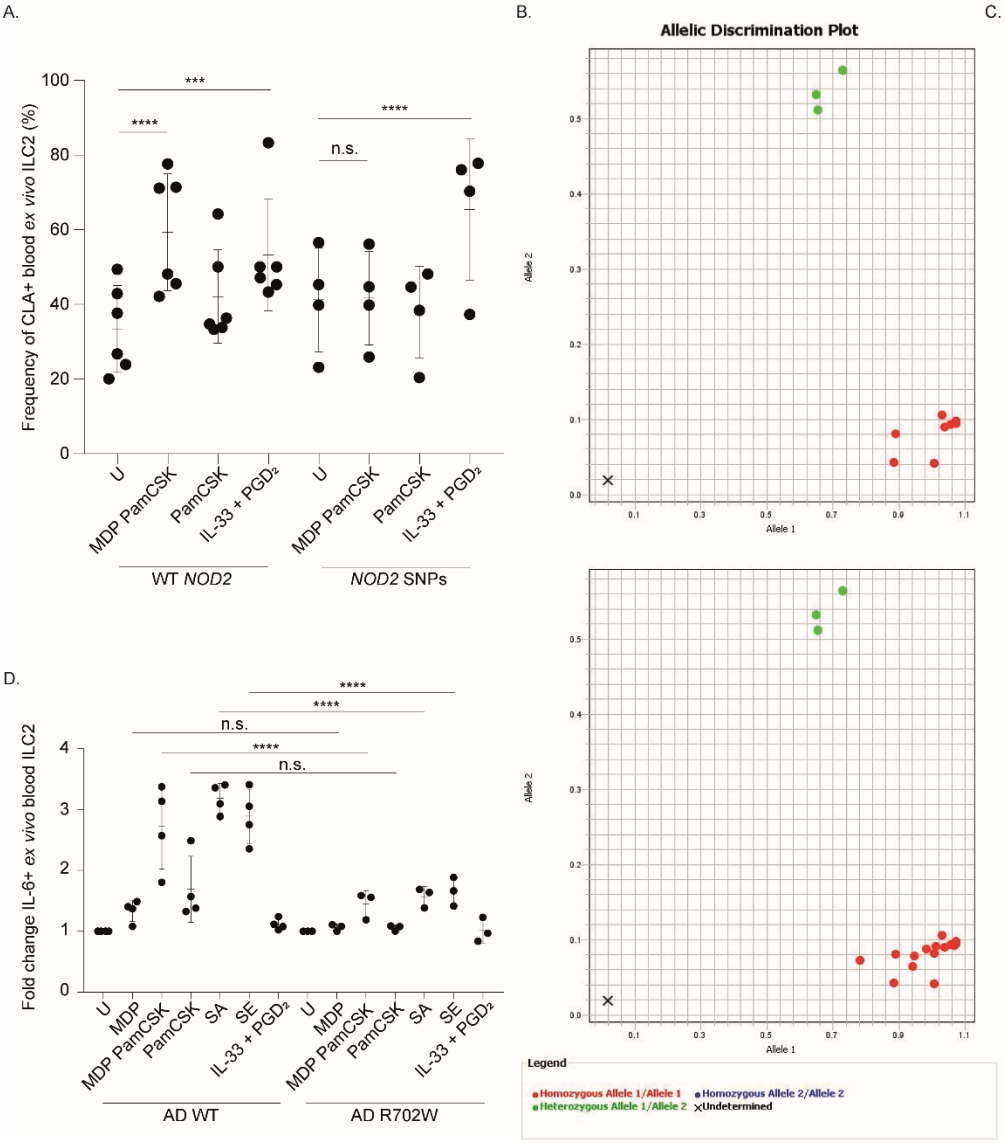

C.

Sample	R702W
HC1	WT
HC2	WT
HC3	WT
HC4	WT
HC5	WT
HC6	WT
HC7	WT
AD1	WT
AD2	WT
AD3	WT
AD4	Het
AD5	Het
AD6	WT
AD7	WT
AD8	WT
AD9	WT
AD10	WT
AD11	Het
DNA blank	Undetermined

Figure S6. ILC2 NOD2 mutation analysis. A. CLA ILC2 surface expression measured by flow cytometry following 24 hour stimulation with MDP (1µg/ml), Pam_3CSK_4 (10µg/ml), IL-33 (50ng/ml) or PGD_2 (100nM), in PBMC from healthy volunteers with wild type *NOD2* gene expression (WT *NOD2*) or patients with loss of function *NOD2* mutations (*NOD2* SNPs). (n=4-6, two-way ANOVA with Dunnett's multiple comparison test, data representative of at least 6 independent experiments). **B.** Allelic discrimination plots of R702W mutation *NOD2* Taqman

genotyping assay of AD patients (upper plot n=11) and total samples (lower plot n=11 AD patients and n=7 healthy volunteers). **C.** Table of genotyping results for R702W mutation *NOD2* Taqman genotyping assay. **D.** Induction of ILC2-derived IL-6 following 24 hour stimulation with MDP (1µg/ml), Pam_3CSK_4 (10µg/ml), heat-killed preparations of SA (*S. aureus*), SE (*S. epidermidis*) or IL-33 (50ng/ml) and PGD_2 (100nM), measured by intracellular flow cytometry in PBMC from atopic dermatitis (AD) patients with heterozygous R702W mutation or wild type (WT) *NOD2* alleles. (n=4 WT and n=3 R702W), one-way ANOVA with Sidak's multiple comparison test, data representative of 2 independent experiments.

Figure S7.

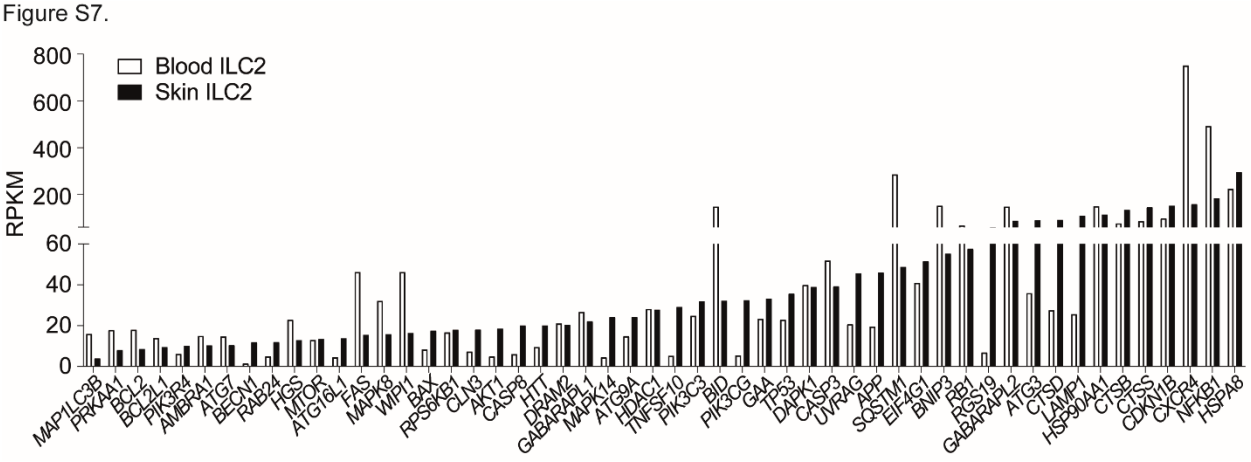

Figure S7. Skin and blood ILC2 may be capable of autophagy. Autophagy-associated gene expression of skin blister and blood derived ILC2 determined by RNA-Seq and measured in RPKM following 24 hour HDM blister challenge.

Figure S8.

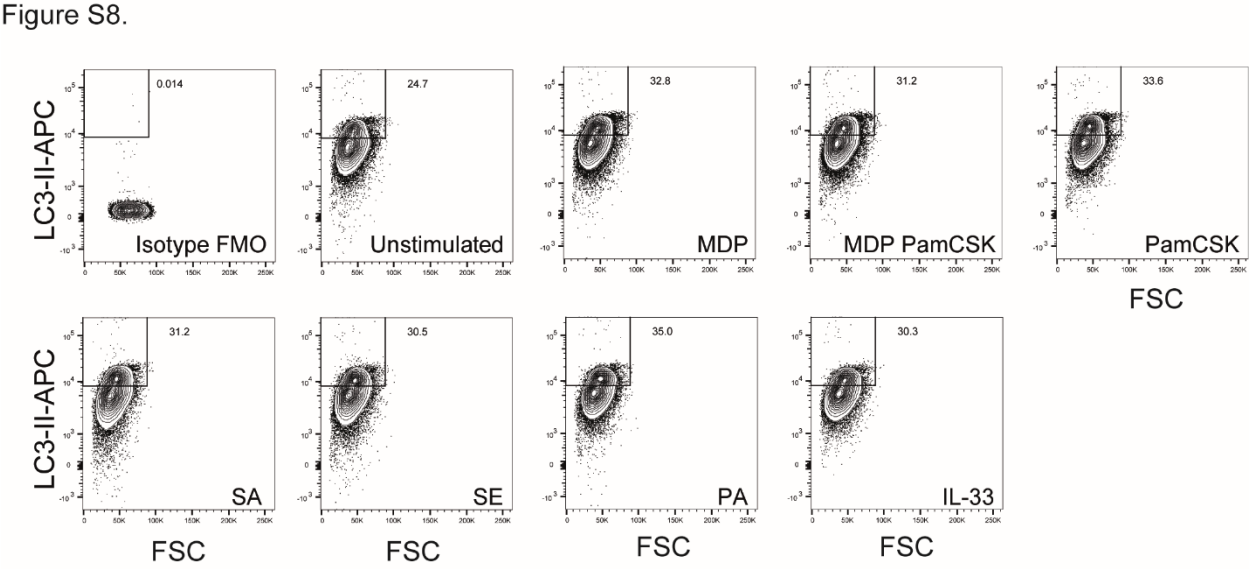

Figure S8. ILC2 LC3-II gating strategy. Isotype FMO control and representative flow cytometry plots gating strategy for detection of ILC2 LC3-II following 24 hour stimulation with MDP (1µg/ml), Pam_3CSK_4 (10µg/ml), heat-killed preparations of SA (*S. aureus*), SE (*S. epidermidis*), PA (*P. aeruginosa*) or IL-33 (50ng/ml) measured by intracellular flow cytometry in ILC2 isolated and expanded from healthy volunteer blood.